A Study on the Failure Mechanism of Permeable Pavement Surfaces

Author:

Sander Zabicki (6027679)

s.zabicki@students.uu.nl

+31637173568

Supervisor Utrecht University:

Tjalling de Haas

t.dehaas@uu.nl

Supervisor Tauw BV:

Floris Harten

floris.harten@tauw.com

A Study on the Failure Mechanism of Permeable Pavement Surfaces

Preface

Before you lies my master's thesis I have worked upon during my internship at Tauw BV. It has been written to fulfill the graduation requirements of the Master of Science, Water Science and Management program at the Utrecht University.

I would like to thank both Ronald Wentink and Annemarie Wolters for the opportunity to write my thesis at Tauw BV. I would like to thank Floris Harten in particular for his substantive and process-based guidance during the past months. Also, I would like to thank my supervisor Tjalling de Haas for his supervision and assistance.

Lastly, I wish to thank my family and friends for their support.

Abstract

Understanding of how permeable pavement surfaces may retain efficient infiltration capacities during high storm water intensities is limited. To evaluate clogging, both performance studies and assessment of permeability for construction quality needs to be assessed. Until now, no earlier research has been conducted where a total population of permeable pavement surfaces were unified into one study.

This thesis combines all usable data of permeable pavement surfaces in the Netherlands. The aim of this research was to increase knowledge regarding the failure mechanism of permeable pavement surfaces and what is causing clogging of the systems. A consistent and improved calculation method is presented that compensates for hydrological variables during experiments.

The rate on which the infiltration capacity of the permeable pavement surfaces is reduced is compared regarding the construction's information. Also, a correlation analysis is conducted to explain individual relationships between various structural elements and low infiltration capacities.

The greater amount of permeable pavement surfaces tested do not function conform the European norm of 97.2 mm/hour. The results show variation in infiltration capacities for each of the studied structural elements. It is concluded that although many permeable pavement surfaces show significant low infiltration capacities, prove of the underlying failure mechanism is limited. This thesis presents recommendations for future research.

Table of Contents

1. Introduction

As a result of climate change, the potential for surface water flooding and its impacts on people, environment, and the economy in the future is likely to grow (Intergovernmental Panel on Climate Change, 2007). The reason for this increase in vulnerability to floods is the increase in rain intensities during storm events. Many studies have proven that due to climate change, the seasonal temperatures are most likely to increase and with that, storm water patterns change. Namely, the amount of water vapor that can be stored within the atmosphere is dependent on the temperature of the atmosphere. The higher the atmospheric temperature, the larger the distance between individual atmospheric particles is, and thus more water vapor can be stored, which vaporizes due to the energy of the sun. When cool air mixes with relative warm air that contains water vapor in the form of clouds, the moisture in the atmosphere can suddenly condense causing large volumes of water to precipitate (Trenberth et al., 2003). Intensities during storms can therefore be severe, especially in summer when temperatures are highest. During storms, most cities rely on large sewerage systems beneath the surface for storm water drainage (Cipolla et al., 2016). Many existing sewers are at or beyond their capacity to facilitate storm water and climate change may, due to higher atmospheric temperatures, increase the volumes of rainfall that occur and therefore also the risk of flooding from sewers (Shaffer, et al., 2009). This calls for climate adaptation strategies. A traditional strategy would be to increase the sewer systems with larger pipe diameters which enhances the discharge capacities and buffer sizes. However, since these systems are relative unsustainable and expensive to implement and maintain, among others due to the fact that they are subterranean, other measures capable to handle the large volumes of water may seem attractive.

Sustainable urban drainage systems (SUDS) have therefore gained growing public interest in recent years, as a result of the positive effects on water quality and quantity issues and other

benefits perceived in the urban area (Qianqian, 2014). The principle behind SUDS is that drainage of (storm) water is managed in a sustainable manner, using technologies that minimize environmental impacts of human lifestyles, buildings, structures and surfaces (Kader, 2015). SUDS are increasingly adopted by municipalities and city councils as they aim to create a safe but also sustainable urban environment. Many of these projects have proven to be great adaptation strategies to reduce urban water stress during storms. However, these measures, such as swales and storm water retention zones, often seize space which is valuable in urban environments. Yet, there are measures that can be implemented without occupying additional space as they can be constructed within combination of other applications. One such measure is the implementation of a permeable surface, as permeable pavement surfaces can be constructed within streets, instead of traditional pavement surfaces. *"Pervious pavements allow stormwater to filter through voids in the pavement surface into an underlying rock reservoir where it is temporarily stored and infiltrated into the surrounding materials. While pervious pavement designs may vary, they all have a similar structure consisting of a surface pavement layer with an underlying reservoir layer."* (California Department of Transportation, 2014, p 2). This thesis explains the research on the performance of permeable pavement surfaces regarding infiltration capacities after implementation.

2. Literature review

This chapter summarizes the literature regarding permeable pavement surfaces and their performances at the time of (simulated) storms. First, general information of permeable pavement surfaces is given. Secondly, contradictions within literature and engineering reports are discussed. The chapter ends with a description of the theory and hypotheses that will be used to guide the research into answering the research question.

2.1 General information on permeable pavement surfaces

A permeable surface is a pavement surface composed of either a structure made with permeable bricks, — although this variant is not very broadly implemented — or (standard) pavers with extended fillings, containing more space between the individual pavers, made out of pervious materials such as soil, gravel, or grass (Cipolla et al. 2016). There are also cases where the permeable surface is constructed with the use of both porous bricks and paving joints which allows the water to infiltrate. Permeable pavement surfaces have considerably different design objectives and requirements compared with conventional pavements and are often used as an alternative to conventional hard impervious surfaces, such as roads, car parks, footpaths and pedestrian areas (Lucke et al., 2014). These systems are specifically designed for the infiltration of storm water through the paving and underlying base structure where it is filtered through the various layers (Boogaard et al., 2015). Reducing the peak flows of storm water by using permeable surfaces for the purpose of water infiltration will therefore help to mitigate against the effects of climate change (Shaffer et al, 2009). After storm water finds its way through the permeable surface, it may infiltrate into the lacing underneath the pavement, see Figure 1. This lacing is, just like the permeable joint fillings, made out of coarse material allowing water to infiltrate. Underneath the

lacing, a coarser material is constructed. This relatively thick layer with its large pores serves as a temporal buffer during storms and is placed on top of the base of the structure or bare soil. A geofabric between the lacing and the buffer layer is occasionally used to prevent materials from the lacing to settle into the buffer layer, making the construction sturdy and prevents pollution of the soil filtering organic and un-organic material coming from the surface (Lucke et al., 2013). During storms (and after), storm water within the final layer of the structure is allowed to seep into the ground beneath or is redirected with the use of drains. The order in which storm water can seep into the soil, is dependent on the characteristics of the soil, whether it is sand, clay or another substance, also known as hydraulic conductivity or K-value in meters of infiltration per day (Fitts, 2013). It is necessary to understand the difference between infiltration rate and infiltration capacity, since these two can easily be mistaken. Infiltration rate is the rate on which a liquid does infiltrate into a porous media at a given time. This rate may vary over a certain period and depends on several factors such as the amount of liquid that is available for infiltration. Simply said, when there is no liquid there is no infiltration. Infiltration capacity however, is more related to the characteristics of the solid and defines the maximum amount of liquid that may infiltrate into a porous media per unit of time. That being said, the infiltration rate can thus not exceed the infiltration capacity.

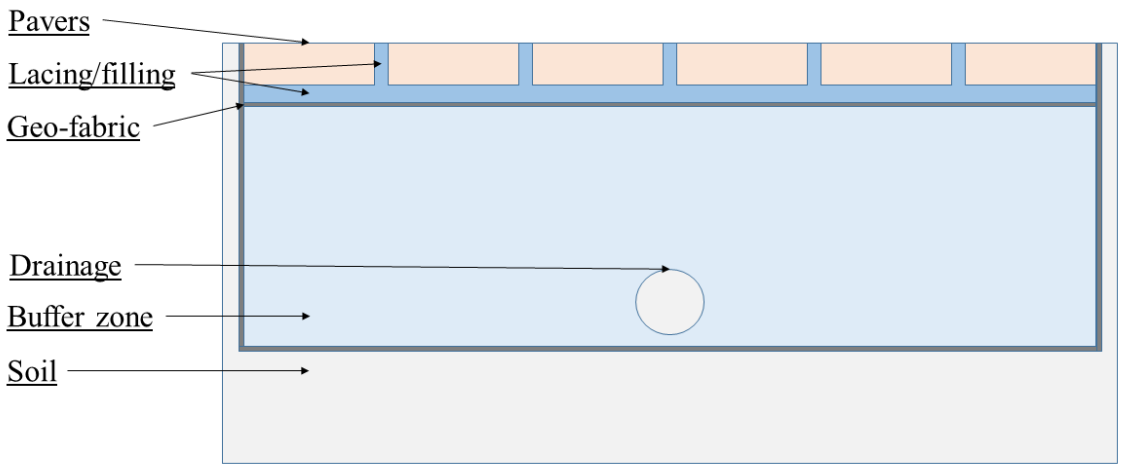

Figure 1: Illustration of typical permeable pavement structure.

A permeable pavement surface must be capable of infiltrating storm water with a minimum rate of 270 liters per second per hectare (L/s/ha), the standard unit used for such applications. This is the minimum European infiltration capacity of 97.2 mm/hour for the Dutch pavements, assuming a 4:1 impermeable to permeable ratio for the catchment area (Lucke et al., 2013). This is equal to a storm event which occurs only once in thirty years for a duration of ten minutes (Beeldens et al., 2006). Usually, a factor 2 is considered during the design of the permeable surfaces, taking future clogging into account (Wegenbouw, 2008). Therefore, for the Netherlands and most of Europe, usually the design of the permeable pavement surfaces is such that the minimum average infiltration capacity of all elements after construction is 540 L/s/ha (Lucke et al., 2014). Since the implementation of permeable surfaces has many benefits, constructing new or replacing already existing roads with permeable pavement is an advantageous method to reduce water stress during storms in urban environments compared to traditional methods. But unfortunately the functioning of this type of measure is not always guaranteed. Namely, after construction various types of permeable surfaces do not contain their infiltration efficiency and drops in infiltration rates are noticed after a certain time (Castro et al., 2007).

2.2 Failing permeable pavement surfaces

The performance of permeable pavements may be hindered because of their life-span, the maintenance needs and even their seasonal performance. Previous studies have investigated infiltration capacities of permeable pavements and in many of the cases results show that the type and age of system and type of joint filling have a significant effect on the long-term hydraulic performance of infiltration systems (Al-Rubaei et al., 2013; Cipolla et al., 2016). Kumar et al. (2015) studied the performance of a permeable pavement surface for a period of four years and found only a marginal decline in infiltration rates of the surfaces after one year of use. However, between years two to four, the infiltration rates declined significantly due to clogging of pores either by dry deposition of particles and/or shear stress of vehicles driving and degrading the permeable surfaces (Kumar et al., 2015). Other studies show that permeable surfaces show significant clogging of the filling material and thus show reduced infiltration capacity just after implementation due to factors such as poor design and traffic during construction (Boogaard et al., 2015). This is supported by Shaffer et al. (2009) who showed that the main source of clogging is construction traffic compressing mud and dirt into the surface, contractors spilling dirt on the completed surface, and inappropriate landscape design that allows dirt to be washed from sources like flower beds onto the surface (Shaffer, et al., 2009). Boogaard et al. (2014) stated that clogging is a result of fine, organic matter and traffic-caused abraded particles, blocking the gaps and surfaces of permeable pavement systems, due to physical, biological and chemical processes and subsequently decreases in the permeability of the surface (Boogaard et al., 2014).

In addition to what is explained in literature, engineering companies acknowledge the complications that have been described. Already considerable amounts of engineering reports discuss the functioning of permeable pavement surfaces where research has been done regarding

infiltration capacities. In many of these studies, clogging happens to be a well-known issue making it unclear how long permeable surfaces remain efficient, maintaining sufficient infiltration capacities (van Oosterwijk et al., 2015; Wentink, 2016; Stamsnijder, 2017). But despite the considerable amount of engineering reports, until now no absolute conclusions have been made regarding the relation between construction types and clogging.

The performance of permeable surfaces is not only determined by the construction as a whole, but also the individual performance of the separate elements — for example due to their difference in porousness. Clogging may therefore also appear on various layers within the construction, which differ for each of the construction types used within the field. Due to the various types of permeable pavement surfaces produced and used in the field, some might be better resilient against clogging than others. Many of these studies explain the issue — some more in-depth than others — but none, however, discuss the definite mechanism that is likely to causes clogging and infiltration rates to decrease. As further research performed on loss of infiltration capacities is relatively limited, determining whether there is a driving factor within the construction that causes clogging seems therefore complicated.

2.3 Complications in previous research

Shaffer et al. (2009) stated that permeable surfaces do suffer a loss of permeability as the gaps in the surface fill with dust and other particles, but that clogging is very rarely sufficient to stop water draining through faster than it falls onto the surface (Shaffer, et al., 2009). So, although permeable surfaces show reduced infiltration rates due to clogging, systems still have sufficient capacities to meet the required permeability of 270 L/s/ha. Shaffer is supported by Lucke et al. (2014) who

states that number a of studies have shown that even visually clogged systems can still demonstrate satisfactory infiltration rates through the pavement surface (Lucke et al., 2014).

However, the outcome of a research is greatly determined by the method that is followed and the location where the experiment has been executed. For example, data from earlier mentioned literature and engineering reports is obtained in several ways with a variety of experimental methods. Each variety has its own pro's and con's but, most importantly, the data being generated during the experiments varies for each separate method. This is noted as Lucke et al. (2014) explains that a variety of infiltration test procedures have been performed in the past, but the results have generally been inconsistent and have shown a large variation in the range of infiltration rates measured (Lucke et al., 2014). This means that conclusions made during these studies remain more or less bound to one location/scenario, specifically. Kumar et al. (2015) do support this as they explain that location is determining the degree on which infiltration rates decline as he found that a decline was mostly observed in driving areas of the parking lots (compared to parking slots, where minimal wear and tear are expected) (Kumar, et al., 2015). In addition, Cipolla et al. (2016) has proven that the infiltration capacity of permeable surfaces differ even on a very local scale, only several meters apart (Cipolla et al., 2016). During the research of Cipolla et al., infiltration rates were measured with a double ring infiltrometer test on three locations, each within one parking space, on a total of eight sites. The results showed that the permeability of the surface was highly affected by the location on which the experiment was performed, see Figure 2. A correlation can be noticed between the permeability and the distance from the road where 'A', close to the road, shows a significant low infiltration capacity relative to 'C', further from the road. This is likely because this position is more influenced by vehicular traffic (Cipolla et al., 2016). The local infiltration rates can show an over- or underestimated value

relative to the entire structure. Conclusions made during previous studies may therefore not be representative of real large scale conditions. Whether entire permeable pavement surfaces still meet the minimum required capacity thus remains unknown, because conclusions relate to only local conditions. These experiments may however provide important knowledge on a small scale, but the interest of municipalities is not per se the infiltration capacity locally but more so the performance of the structure as a whole.

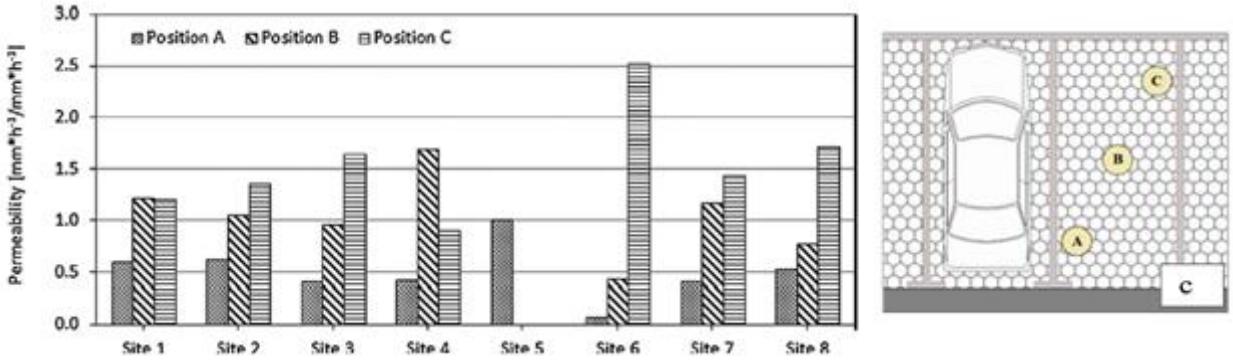

Figure 2: Correlation between the position of the ring in the stall and (Cipolla et al., 2016).

In 2014, a report was published by Lucke et al. (2014) describing a new experimental test to determine the surface infiltration capacity of permeable pavements. As the number of permeable pavement surfaces increases, the need for an appropriate tool to measure their surface infiltration functionality as a whole was desired, especially with respect to clogging (Lucke et al., 2014). Figure 3 shows an illustration of the double ring infiltrometer and the full-scale test. The 'improved' full-scale method is a large scale experiment where, over a relatively large area, the infiltration rate is being calculated, based on the measurement done. During the falling head full-scale (FHFS) method, the pavement surface of interest is inundated until the water level reaches near its maximum (the curb or speed bump). Once this level is reached, the water supply is stopped and the time needed to drain the permeable pavement surface is noted. During the constant head full-scale (CHFS) method, the pavement surface is inundated until a certain water level and the water

level is subsequently kept constant around this point. When constant, the discharge/applied flow rate is being measured (Lucke et al., 2014). A brief description of the full-scale method, as well as the double ring infiltrometer test, is given in Appendix 1.

Lucke et al. concluded that the infiltration rates regarding the double ring infiltrometer and the full-scale test were different, but not significantly. Both methods are considered satisfactory for determining the infiltration capacity in the Netherlands. However, since literature describes relative large local differences between infiltration rates measured with the use of the double ring infiltrometer, conclusions made during the evaluation of the full-scale method in Lucke's et al. (2014) report can be doubtful. This is supported by what is seen in engineering reports discussing results of both full scale and double ring infiltrometer experiments. Infiltration capacities calculated with the full-scale test currently tend to be more convenient than those of the double ring infiltrometer method. But, even though the full-scale test may seem more promising, results from previous studies have still generally been inconsistent and showed large variation in the range of infiltration rates measured. Therefore, also this method remains questionable. One possible reason is that during experiments, storms have been simulated unrealistically due to the use of high water columns.

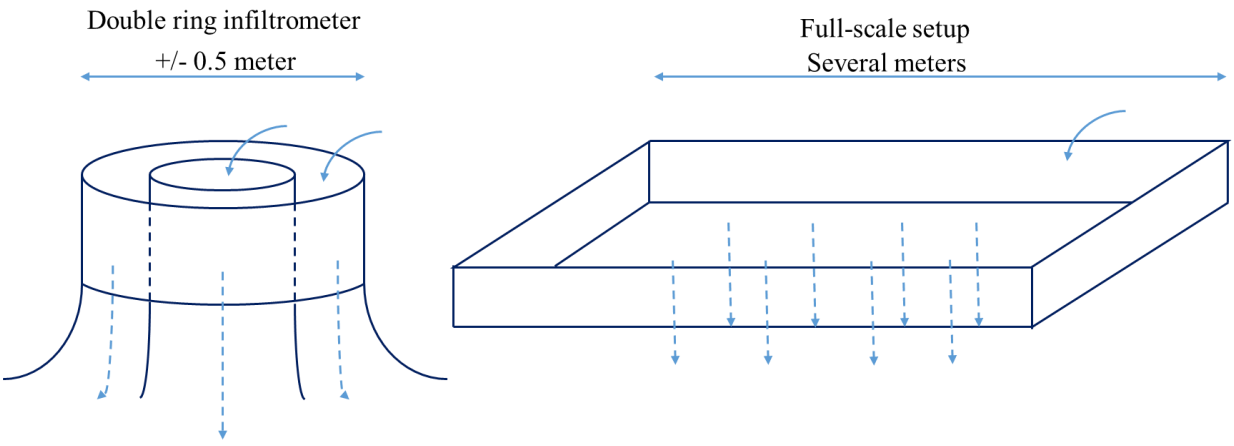

Figure 3: Illustration experiment methods, left; double ring infiltrometer test, right; full-scale test.

2.4 Hydrological variables

The permeability of a porous media is described by Darcy's law:

$$\frac{Q}{A} = \frac{k\Delta p}{\mu L}$$

Here, Q is the discharge over a certain area [m^3/s], A is the area [m^2], k is the permeability [m/s], Δp is the pressure drop on top of the surface [Pa], μ is the fluid viscosity [Pa·s], and L is the thickness of the porous media [m]. The infiltration rate of the permeable surfaces is thus dependent on the pressure head of the water column (Fitts, 2013; Nortier et al., 1996). The higher the water column due to storm water, the higher the pressure is at the surface, see Figure 4. Infiltration rates calculated with the CHFS method are based on experiments where a certain relatively high pressure head (water column) is maintained. Also, during the FHFS method, the initial pressure head is relatively high. Although, these simulated water columns might not be representative for real events. In reality, the water column due to storm events spreads somewhat evenly over time and should stay relatively low. Because computations of the infiltration rates during the FHFS and CHFS were done with a relative high pressure head at the pavement surface, results might therefore be overestimated. The fact that Shaffer et al. (2009), and Al-Rubaei et al (2013) claim that infiltration capacities still remain sufficient after years, might not be true for other water columns used during experiments. Infiltration rates during storms may therefore actually be less and might even be under the described norm of 270 L/s/ha. In addition, other hydrological variables such as the water content of the porous media, are determining the permeability of porous media (Fitts, 2013; Nortier et al., 1996).

$P = \rho * g * h$	$[kg/m/s^2]$	$(pressure)$
$\rho = 1000$	$[kg/m^3]$	$(density\ of\ fresh\ water)$
$g = 9.81$	$[m/s^2]$	$(the\ Netherlands)$
$h = pressure\ head$	$[m]$	

Figure 4: Illustration of pressure head on pavement surface.

In the infiltration process water enters the surface due to the combined influence of gravity and capillary forces (Gray et al., 1967). Both forces act in the vertical direction which cause percolation downward into the surface and through the porous media. The permeability or hydraulic conductivity is the maximum amount of meters a liquid can flow through porous media per unit of time. As the order in which storm water infiltrates into the permeable structure may be influenced by the hydraulic conditions present during the tests. It is therefore important to investigate the sensibility of hydrological variables during the experiments such as the water table used and the effect it has on the infiltration rate.

Similar to the flow through a saturated porous media, water flow through an unsaturated porous media is generally governed by Darcy's law (Zhan, 2004). However, there are two major differences. Firstly, there is a storage within pores which represents the variation of water content with matric suction and secondly, the water coefficient of permeability depends strongly on matric suction.

Water content and matric suction

The water storage within pores is causing variations in matric suction of porous media (Nortier et al., 2996). The main cause for this difference is the amount of water that is present within a porous media, since this is affecting the pore water pressure or matric suction (Fitts, 2013). Water

molecules are attracted to other water molecules. This phenomenon is called cohesion. Water molecules are also attracted to other fluids or solid surfaces. This is called adhesion. Adhesion is the result of surface tension. Surface tension is the attraction of molecules of one kind for molecules of a different kind due to a difference in polarity (Kalmikov, 2010). As is illustrated in Figure 5, water particles are attracted not only to other water particles, but also to solid surfaces like for example mineral grains. The water molecules will 'stick' on the solid's surface due to forces caused by surface tension. The order on which water is attracted to a solid surface depends on the type of material, but also on the dimensions of individual pores. Substances with a higher surface tension, have stronger forces between the molecules together. It is these forces that cause matric suction and so the water pressure present within pores to be negative relative to atmospheric pressure. Due to this negative pressure, the matric suction is therefore influencing the amount of storm water that may percolate.

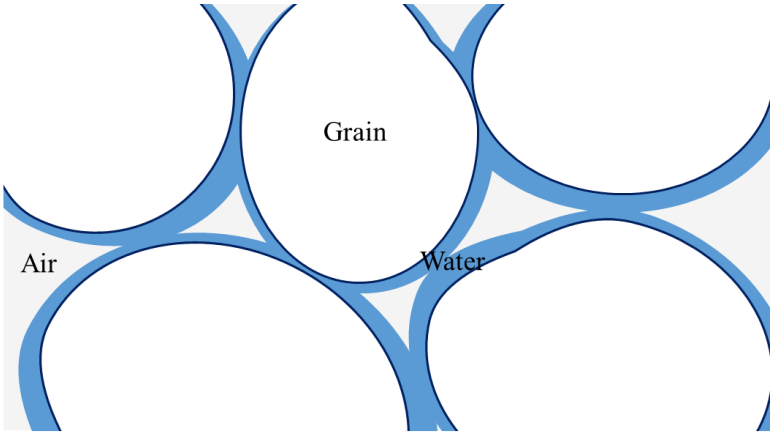

Figure 5: Illustration of the effect of surface tension, based on Fitts (2013).

The pore water pressure is caused by what is called capillary forces and is the result of adhesion between water and a solid surface (Fitts, 2013). The capillary force within pores can be described by the following equation (Finn, 1999);

$$F = 2\pi r T Cos\theta = \rho g(h\pi r^2)$$

where *F* is the capillary force, *T* is the surface tension, *Cosθ* is the angle of contact, *r* is the radius of the pore, ρ is the density of the fluid, *g* the gravitational acceleration speed (9.81 for the Netherlands) and *h* is the water height. The equation explains that there is an equilibrium between the force due to surface tension and the gravitational force of the volume of water. The equation can be rewritten so that the effect of the pore suction can be calculated;

$$h = \frac{2TCos\theta}{\rho g r}$$

where *h* is the total height water gets sucked into a pore. In Figure 6, the matric suction of a pore is illustrated as a capillary tube representing a single pore with size '*2r*'. In the figure, a certain volume of water is pulled upwards due to the capillary forces caused by surface tension between water and glass. In this figure, the capillary forces are illustrated as '*F'*. It is the relation between the radius and the volume, with its gravitational forces, that determines the suction and thus the height of the pore water table.

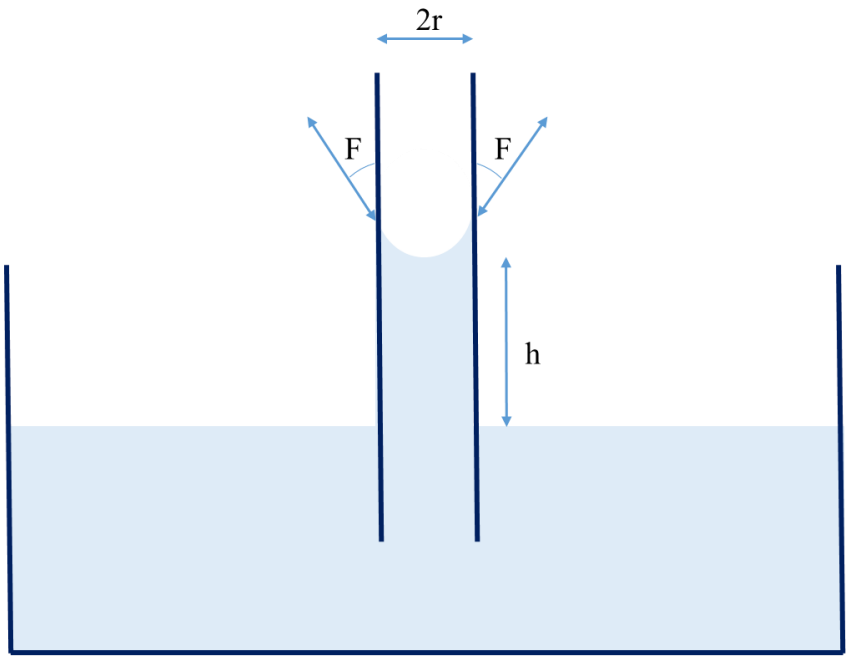

Figure 6: Illustration of capillary forces resulting in matric suction, based on Szymkiewics (2013).

Depending on the radius of the tube, the water table *h* is pulled high or low relative to the initial water surface. From the equation it can be made clear that a radius twice as small will result in a water table to be pulled upwards double the height. Larger radiuses therefore causes the water pressure to be less significant than pores with a smaller radius. Vice versa, *h* is relatively large for small pore sizes since due to surface tension their negative pressure (negative relative to atmospheric pressure) is greater in respect to gravitational forces pulling the water downwards.

During the saturation process of a porous media, the matric suction changes over time (Zhan, 2004). In dry conditions, the matric suction is highest as the amount of empty pores is at its maximum. As small pores have a large capillary force, it is mainly these smaller pores to become saturated first if (storm) water is added to the porous media. While the porous media becomes more saturated, the strength on which water is absorbed by a porous media becomes less. Not only the amount of unsaturated pores is decreasing but also because mainly larger pores will remain,

having less matric suction. Figure 7 visualizes this ratio. It shows the volumetric water content over matric suction for a sandy and clayey soil. In this figure, a high water content relates to low matric suction and the other way around.

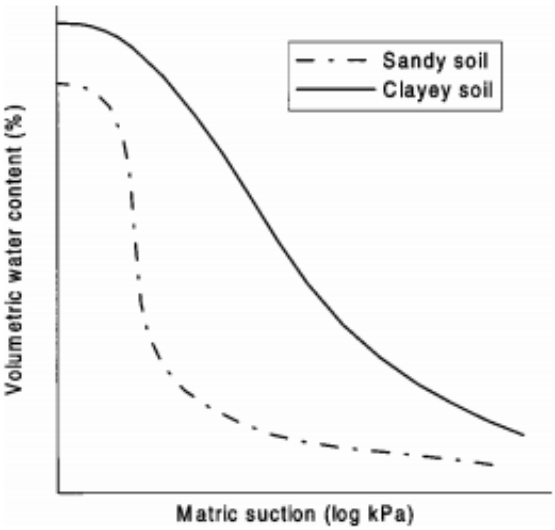

Figure 7: Soil–water characteristic curves for different soils (Zhan, 2004).

Horton (1941) is supporting the fact that infiltration rates drop over time in case water is constantly submitted (Horton, 1941). Horton is the founder of following equation;

$$f = f_c + (f_0 - f_c)e^{-K_f t}$$

where f is the infiltration rate, f_c is the constant or equilibrium infiltration rate after the soil has been saturated and f_0 is the initial infiltration rate. The empirical equation explains that infiltration starts at a constant rate, f_0, and that this infiltration rate decreases exponentially with time, t. After some time when the soil saturation level reaches a certain (maximum) value, the infiltration rate will level off to the rate of f_c. This f_c is also known as minimum infiltration capacity. Note that this

is not the minimum infiltration rate as this is depending on the amount of water available for infiltration.

Pressure head

As a porous media is becoming more saturated and pores are filled with water, the absorption effect is becoming less and therefore decreases the contribution to the infiltration rate. In the case when the pores are fully saturated, there will no longer be infiltration due to matric suction. The vertical flow through the porous media will then only be because of the result of gravitational forces and pressure differences. Due to gravitational forces and pressure as the result, water will flow from a high water pressure (large water column) towards a lower water pressure (small water column) due to pressure differences. For flow through a porous media, the flow rate on which water will flow from high to low pressure is described by Darcy's law described earlier in this report. For saturated porous media, this equation can also be written as (Nortier et al., 1996);

$$q = -\frac{K\Delta h}{d}$$

where q is the velocity, K is the hydraulic conductivity, h is the potential difference of the water table and d is the depth (or length) of the porous media.

Within the construction of a permeable pavement surface, multiple layers have been constructed with different materials each having its own permeability. The vertical flow of each of the individual layers is determined by Darcy's law according to following equation (Nortier et al., 1996);

$$q_i = -\frac{K_i\Delta h_i}{d_i}$$

where K_i is the hydraulic conductivity in a layer, h_i is the head drop in a layer and d_i the thickness of a layer. But although the K-value of each layer can be different, the layered system can be represented as one homogeneous anisotropic layer with one value of hydraulic conductivity which represent the overall vertical resistance to flow (Fitts, 2013). This is explained by following equation (Fitts, 2013);

$$q_z = -K_{ze}\frac{\Delta h}{\Delta z}$$

with q_z being the vertical specific discharge, K_{ze} the vertical equivalent conductivity. The vertical equivalent K_{ze} is explained by following equation (Fitts, 2013);

$$K_{ze} = \frac{\sum d_i}{\sum(\frac{d_i}{K_i})}$$

2.5 Problem definition and research aim

Future storms with high rainfall intensities can cause significant amounts of water to fall and run onto permeable pavement surfaces. If due to clogging the infiltration capacity of the permeable surfaces is exceeded by the storm water intensity, water starts to build up creating ponds and may even cause floods. It is in the interest of municipalities and cities to prevent nuisance and flooding due to extreme events, but permeable pavements are a relative new technology and scientific research done on their performance is limited. The main cause of clogging — and the factors that tend to enhance the effect of clogging — are yet not broadly or scientifically investigated and discussed. Recommendations to be considered at planning and construction to guarantee a long lifecycle of the systems are therefore not well described.

Study on literature and the engineering reports discussing the infiltration capacity of permeable pavement surfaces explain that there are complications regarding clogging of the

systems. In order to assess the reduction in infiltration rates which occur over time due to clogging, various test procedures have already been utilized in the past. However, the results have been inconsistent and show a large variation in infiltration rates measured. The little research done on permeable pavement surfaces and the fact that experiments or calculations have been executed in numerous ways renders the causes of clogging poorly understood. Thus, understanding of how urban environments may retain efficient resilience against the effects of climate change on the increasing threat of storm water by the implementation of permeable pavement surfaces is limited. But, as the use of permeable pavement surfaces increases, a definitive test method is needed to measure hydraulic performance (Li, 2013). To evaluate clogging, both performance studies and assessment of permeability for construction quality and maintenance needs to be assessed. The aim of this research is therefore to increase knowledge regarding the failure mechanism of permeable pavement surfaces and what is causing clogging of the systems by analyzing existing data created during previous experiments, with both a consistent and improved method, regarding specific construction- or soil characteristics. The research question that will be answered during the research remains is as follows:

Is there a correlation between the magnitude of failure and failure mechanism of permeable pavements?

In this context, failure is when is a permeable pavement surface is un-capable of maintaining sufficient infiltration capacity to comply with the European norm of 97.2 millimeter per hour. In order to come to an answer to the research question, the following sub-questions are considered:

A. *How significant are infiltration capacities after hydrological variables are taken into account?*

B. *Do different types of permeable pavement surfaces show significant reduced infiltration capacities?*

2.6 Hypotheses

Literature describes that, until now, various methods have been used to determine the infiltration capacity of permeable pavement surfaces. Some authors claim that systems show rates after several years of implementation sufficient to meet the norm of 270 L/s/ha. The infiltration rate is determined by factors such as hydrological variables, for instance pressure head and water content. It is assumed that the results during previous studies have been inconsistent and might even been exaggerated, showing unrealistic results. Therefore, a 'new' data analysis on the already existing data may lead to relevant conclusions on behalf the performance of permeable pavement surfaces. This study hypothesizes that with realistic hydrological variables during simulations, infiltration capacities show reduced values relative to current values. This is further described as 'H 1'. Corresponding null-hypothesis is that the pressure head has little effect on the infiltration rates and that infiltration capacities found during previous studies are sufficient for further research.

Soils with small pores allow only slow migration of water while materials with larger, less constricted pores permit more rapid migration (Fitts, 2013). The porous area/volume of the permeable pavement surfaces (construction type) is thus determining the speed on which water infiltrates, but may also influence the speed on which debris clogs the system. This porousness is different for specific types of permeable pavement surfaces and is based on the type of pavers, fillings and lacings materials. Therefore, different types of constructions may show significant

lower infiltration capacities than others. The second hypothesis of this research is that the type of permeable pavement surface is determining the order on which the structure shows effects of clogging as reduced infiltration capacities. This is further described as ‘H 2’. Consequently, the null-hypothesis is that the type of permeable pavement surface does correlate with the reduced infiltration rates. The conceptual framework of the theory is displayed in Figure 8.

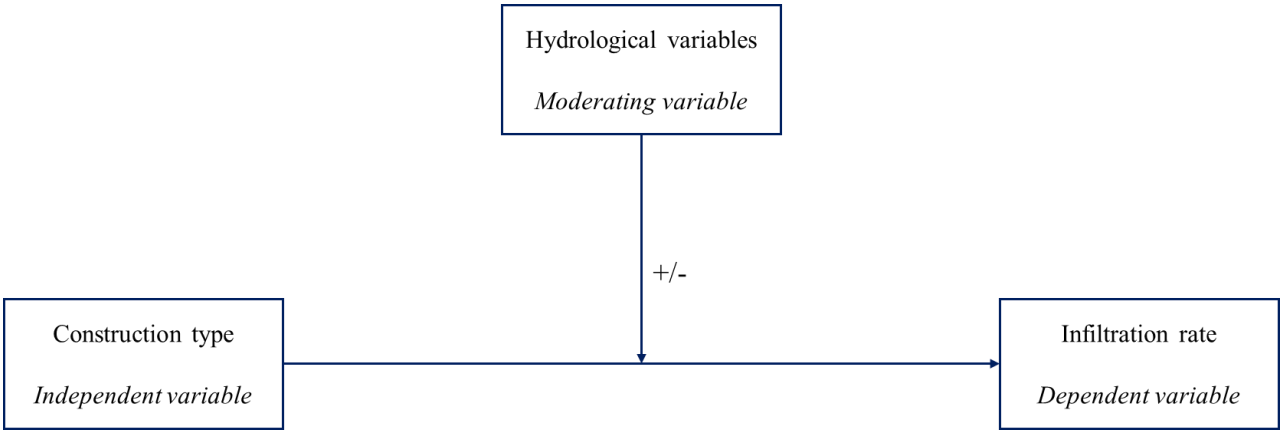

Figure 8: Conceptual framework of research. In this figure, the independent variables are various construction types with each having their own design characteristics. These construction types have their own individual infiltration capacity. These infiltration capacities can be studied with experiments and are influenced by the type of construction/structural elements. The hydrological variables during the experiments influence the outcome of the experiments. Therefore, these are named moderating variables.

3. Methods

The research question, as well as the sub-questions were answered conform the method that is described in this chapter. The elements from the method are presented in the flow diagram, as seen in Figure 9. First, data was collected. Secondly, the data was used to calculate the infiltration capacities in one uniform manner. Finally, after calculations were done, an analysis was performed. Based on the analysis, recommendations for future implementation of permeable pavement systems were discussed.

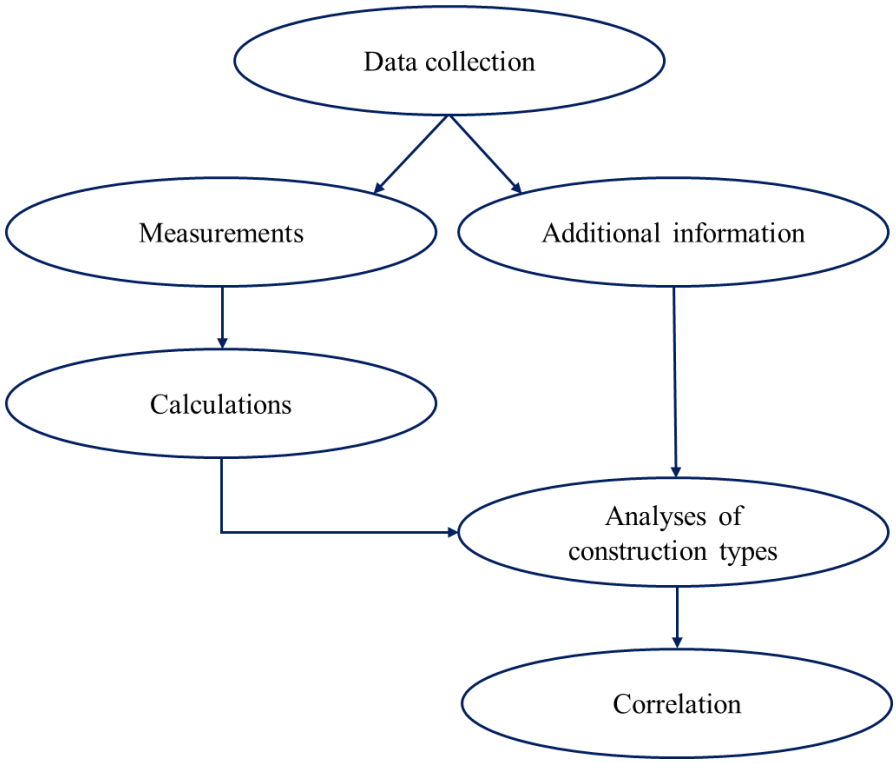

Figure 9: Flow diagram of method.

3.1 Data collection

During the data collection phase, the current available data (previous measurements done by Tauw BV) was gathered and stored. Within a database, only the results produced during previous full-scale experiments (both FHFS and CHFS) were stored (as literature described that this method currently is the most convenient). Furthermore, additional relevant information regarding the construction type/elements, age of construction, soil and environmental characteristics were collected. Additional information relevant for this research was requested by contacting municipalities, cities and construction manufacturers.

Measurements

All data produced during previous experiments performed by Tauw BV in co-operation with municipalities across the Netherlands was obtained. In total, around 30 measurements were done according to the falling head full-scale method. However, only 24 out of these 30 measurements were of sufficient quality to be used in this research. The remaining 6 measurements either showed unexpected results, were done on locations that are not valuable for this research, or were known to be unreliable due to severe leakage. The full list of locations from the included 24 measurements is given in Table 1.

Table 1: Test locations and street names.

#	Test locations	Street name
1	Almere 1	Centaurenstraat
2	Almere 2	Apollostraat
3	Almere 3	Homeruslaan
4	Beverwijk 1	Halve Maan (Noorder)
5	Beverwijk 2	Halve Maan (Zuider)
6	Breda/Effen	Baanakker
7	Delft	Drukkerijlaan
8	Dussen 1	Groot Zuideveld
9	Dussen 2	Groot Zuideveld
10	Egmond aan Zee	Julianastraat
11	Goirle1	Sporenring
12	Goirle2	Sporenring
13	Rotterdam 1	Hoevestraat
14	Rotterdam 2	Harddraverstraat
15	Rotterdam 3	Baljuwplein
16	Rotterdam 4	Hoekersingel (1)
17	Rotterdam 5	Hoekersingel (2)
18	Rotterdam 6	Hoekersingel (3)
19	Rotterdam 7	Hoekersingel (4)
20	Utrecht 2	Brasemstraat
21	Zwolle 1	Pieterzeemanlaan
22	Zwolle 2	Beukenallee
23	Zwolle 3	Groeneweg
24	Zwolle 4	PC Hoofdstraat

During the experiments, the pressure was measured with the use of so called Divers. Divers are little measurement devices which can be used to measure water- and atmospheric pressure and temperature, in addition to other parameters. See Figure 25 in Appendix 1 for a photo of such a device. The data of these devices can be used to calculate the water column over time during the experiments. The equation that is used to calculate this water column is as follows (Eijkelkamp, n.d.);

$$WC = 9806.65 \frac{P_{diver} - P_{baro}}{\rho g}$$

where WC is the water column [cm], P_{diver} is the measured water pressure of the diver [Pa], and P_{baro} is the measured atmospheric pressure of the barometer diver [Pa]. With this equation, each Pa is equal to one millimeter. Preferably, at least two Divers are used to measure water pressure as well as atmospheric pressure. However, not all measurements were done with an additional Diver measuring the atmospheric pressure. It was therefore decided that only the data from the Diver measuring the water pressure was used. Therefore, in upcoming graphs the pressure ranges above the 1,000 Pa, as the atmospheric pressure is still included. During this research it was assumed that the atmospheric pressure remains equal during the experiments and each reduction of 1 Pascal stands for a reduction of 1 millimeter in water column.

Some measurements were done with several Divers for the purpose of validation or excluding the risk of losing data if one Diver malfunctioned during the experiment. During the calculation phase, it was possible to bundle the data provided by these Divers beforehand to create one average dataset for each of the locations. However, this is not always possible since the Divers were placed on different places on the surface. Therefore, the initial water height and thus water pressure during experiment did vary for the various Divers. Also, some Divers did not measure pressure because they became dry, while others were still below the water surface. If the results of both these Divers would be combined, the average pressure would show false values. It was therefore decided that if more than one Diver was used during one experiment, the data of additional divers only served to evaluate the data on quality and was not used for the determination of the infiltration capacity.

Additional information regarding the structure

Secondly, during the data collection, additional information regarding the design and environment of the various pavement surfaces was obtained for each of the 24 locations. The various design and environmental aspects that are included were based on the literature review and based on information from municipalities. The variability in the different elements within the typical structure of permeable pavement surfaces was obtained and linked to the locations. Elements listed below were considered during future analyses. Unfortunately, gaining additional information about the design of the permeable pavement surfaces from the locations in Almere was unsuccessful. During the analyses, therefore, the design and environment characteristics of these three locations are mentioned as 'Unknown'.

- Age

  This category shows how long a construction has been in use in years from the moment it got constructed towards the moment of the experiment.

- Manufacturer

  This category shows which manufacturer has designed/constructed a permeable pavement surface.

- Curved surfaces

  This category shows whether the surface of a construction is curved or not.

- Filling material

  This category shows what filling material is used for the joints of a construction.

- Size of joints

This category shows the total width of the joints in millimeters (between two bricks) and explains the permeable surface of the constructions.

- Type of lacing

  This category shows the material used for the lacing of a structure. Often, this material is the same as the material used for the joints.

- Geo-textile

  This category shows whether a geo-textile is implemented or not.

- Buffer layer

  This category shows what material is used for the buffer layer of a construction. Usually, this material is coarser than the material used for the joints and lacing.

- Soil type

  This category shows the predicted soil type underneath a construction. (Although it is assumed that the effects this has on the infiltration rate of the construction during the experiments is relatively small, the soil type is still taken into account).

- Environment

  This category shows the amount of vegetation that is implemented within the close environment of a permeable pavement surface. Following variables are used;

  Low: no to little green area and lo sized trees

  Med: some green area and medium sized trees

  High: large green area and large sized trees

3.2 Calculations

During the calculation phase, the data was used to compute the infiltration capacities of the permeable pavement surfaces with the use of one uniform calculation method. The calculation method is based on the hydrological variables described in the literature review. The result of this phase is a list of infiltration capacities in millimeter per hour for all permeable pavement surfaces tested by Tauw BV.

Recommendations for calculation phase

During a storm event, a certain volume of precipitation — depending on the intensity of the storm — will end up on the permeable pavement surface. This volume will percolate into the surface and infiltrates through the porous media to the extent possible. The results of the literature review on the effects of the water content of a porous media on the infiltration rate explains that the speed on which water may infiltrate into a surface, is dependent on the water content as well as the water column maintained upon the permeable surface.

The water content of a porous media has a significant influence on the amount of water that may percolate/infiltrate into the media. Literature describes that this is due to capillary forces of individual pores as the result of surface tension between water and solid. Due to these forces, the percolation into the surface is highest in dry conditions and becomes exponentially lower the more saturated the porous media gets. After the saturation process, the discharge, or change in discharge, is no longer affected by the water content as it remains steady. In this case, the infiltration rate is determined by the permeability of the structure and the water height maintained during the experiment.

Because of their importance, the influence of two hydrological variables that was studied and its effects on the outcomes during previous experiments cannot be neglected. This is recognized by studying the results of the past experiments. Below in Figure 10 & Figure 11, two graphs are shown where on the x-axis the time and on the y-axis the measured water pressure is noted. Figure 10 shows the pressure measured on one of the locations in Almere from maximum water height to minimum water height during the experiment. The effect of the water content and or water column is clearly visible. Namely, during the first half of the experiment, between 00:00 and approximately 01:18, it can be noticed that the change in water pressure is not linear but more or less decreasing exponentially. This can be explained by the effect of matric suction becoming less due to the saturation process of the construction and the relative large water column present during the experiment. While the time progresses — and by that the effects of the matric suction and water column is reduced — the change in pressure (which of course can directly be converted to infiltration rate) becomes more or less linear in the second half of the experiment. During previous studies, usually a linear regression line was created for each experiment to determine the infiltration capacity of the construction.

In Figure 11, only the change in pressure during the very last centimeter of the same experiment is shown. By comparing the change in pressure of both these graphs, it becomes clear that the infiltration capacity is significantly less at the end of the experiment in comparison to the total experiment. Namely, in the case for this specific location in Almere, a linear regression line over the total duration of the experiment gives an infiltration capacity which is 134% relative to the one calculated over the last centimeter.

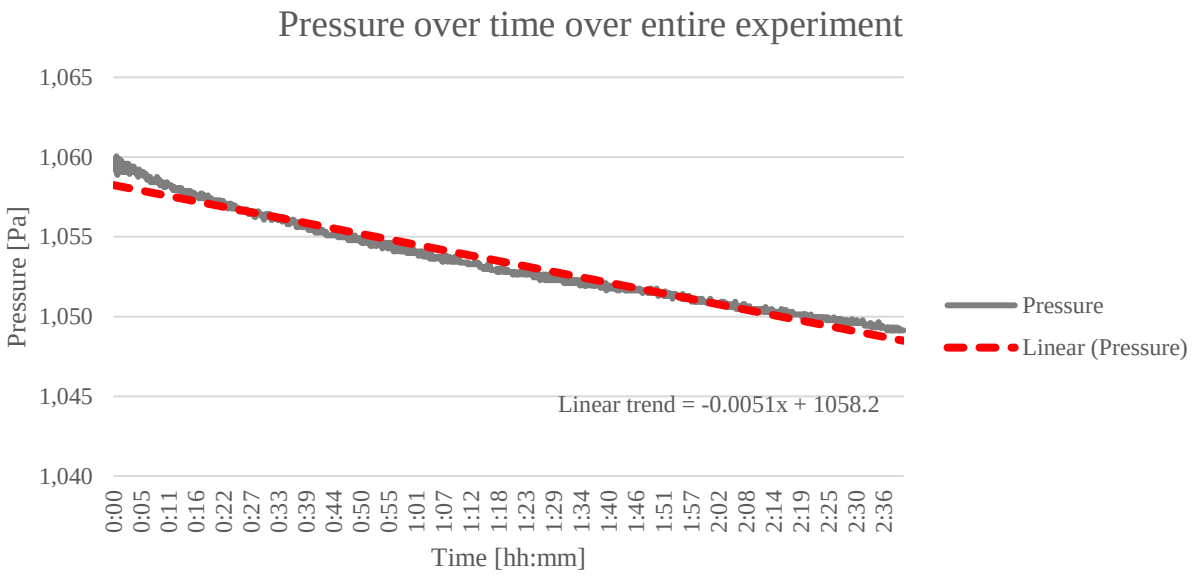

Figure 10: Water pressure during entire range of experiment.

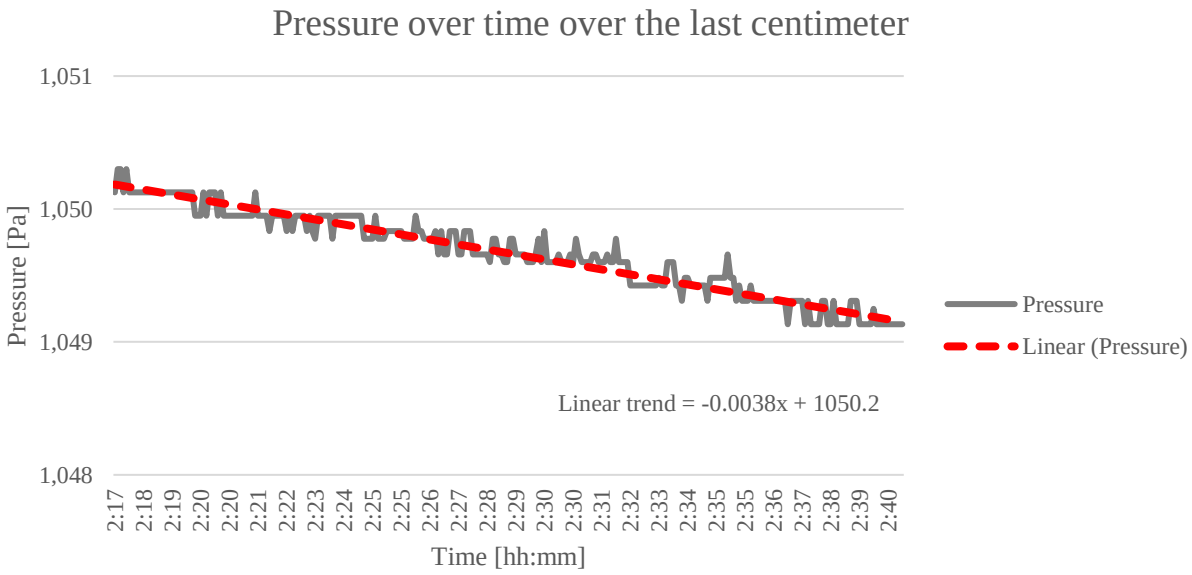

Figure 11: Water pressure during last centimeter of experiment.

The design infiltration capacity of permeable pavement surfaces is, according to the European norm, 270 L/s/ha, which is just over 97 millimeter per hour. This means that the

constructions should have sufficient permeability to resist the traditional (Dutch) design storms T=2 (19.8 millimeter in one hour) and T=100 (60 millimeter in one hour), excluding discharge originating from surrounding area. But often, a greater amount of water originating from the catchment area such as roofs and (paved) patio surfaces is redirected towards the streets. During these storms, the amount of storm water ending up on the permeable pavement surfaces is therefore likely to overshoot the amount required for the saturation process (of course depending on the total catchment area responsible for the discharge). In addition, the structure may still be saturated from previous storm events. So to ensure the effectiveness of the measure in terms of storm water resilience, even in the worst-case scenarios, the infiltration rate must be sufficient even in saturated conditions. Therefore, during the calculation phase an improved method has been conducted where the infiltration capacity of the measure is seen as the infiltration rate calculated within the last centimeter. Since dt/dh is more or less linear in this last range for each of the 24 measures, the infiltration capacity calculated with this new method will give values about equal to Horton's equilibrium infiltration rate 'f_c' (Horton, 1941). The results of this new calculation method show reduced infiltration capacities relative to the ones calculated with method used previously.

As can be noticed in Figure 11, the measured pressure is fluctuating with about +/- 0.1 Pa relative to the trend line. This fluctuation is most likely caused by a changing atmospheric pressure or small disturbances in the water surface, as well as small errors of the measuring equipment. The error of 0.1 Pa over a total is 1.0 Pa seems significant as the errors are about 10% of the total range. However, since the fluctuations are both positive and negative and the linear trend is not influenced significantly by these individual errors, it is assumed that the linear trend over the last centimeter is reliable.

3.3 Analyses of construction types

With the results of previous calculation phase, correlation between infiltration capacities and permeable pavement surface types were studied. The rate on which the infiltration capacity of the constructions is reduced was compared regarding the construction's information. Afterwards, the results were visualized with the use of graphs and tables. Since the calculation method used to compute the infiltration capacity is uniform, the results of this phase were used to conclude whether correlation can be found between failure and failure mechanism.

In addition to the visual analyses, a correlation analysis has been performed with the intention to study the correlation between the various factors. Correlation is the relation between two (or more) things and is the statistic representing of how closely two variables co-vary (Mukaka, 2012). Correlation can be computed with several methods, depending on the type of data. In this case, the data consist of multiple independent variables (design and environment) and one dependent variable (the infiltration capacity). The independent variables consist of both numerical and categorical data. Because the type of data from the independent variables varies, it is not possible to perform a multiple data analysis on the entire range of data with just one method. It is therefore chosen to perform an analysis on each of the independent variables separately to study the individual correlation. Pearson's equation is used to determine the correlation between two variables (Mukaka, 2012). The equation is as follows;

$$r = \frac{\sum(x - \bar{x})(y - \bar{y})}{\sqrt{\sum(x - \bar{x})^2 \sum(y - \bar{y})^2}}$$

where r is the correlation value ranging from -1 to +1, x is the independent variable and y is the dependent variable (Debye et al., 1957; Mukaka, 2012). This function calculates the correlation coefficient between two measurement variables and is used to determine the extent on which one variable determines the change of the other variable and has been used widely since it has been

published by Debye et al. in 1957. With this equation, an outcome of -1 and +1 stands for perfect (reverse) correlation and 0 meaning no correlation at all. In this research, the following scale was used to categorize the correlation of each aspect;

- between 0 and (-) 0.25, no correlation;
- between (-) 0.26 and (-) 0.50, weak correlation;
- between (-) 0.51 and (-) 0.75, moderate correlation;
- between (-) 0.76 and (-) 1.00, strong correlation.

4. Results

4.1 Data collection

In Appendix 2 you can find the results of the data collection. Within the appendix, all information found during the data collection is listed per permeable pavement surface included in this research.

4.2 Calculations

According to the recommendations described in the methods section, calculations have been performed with the use of an improved method. This is done by calculating the slope (dt/dh) of the data points for the last centimeter for each of the 24 locations. The results of these computations are given in Table 2. For each of the 24 locations, the infiltration capacity is given in millimeter per hour. The infiltration capacity ranges from 10.1 millimeter per hour (lowest) to 248.4 millimeter per hour (highest) with an average of 88.5 millimeter per hour. On average, the infiltration capacity of the permeable pavement surfaces tested is below the European norm with some surfaces showing more than twice the capacity, where others show only as little as 10 percent. Overall, the infiltration capacity varies greatly between the various pavement surfaces, where on eight locations the permeable surfaces showed infiltration capacities that still were sufficient according to the European norm. The other sixteen surfaces did not. In Figure 12 a visualization of the results in comparison with the European norm is shown.

Table 2: Calculated infiltration capacity over the last centimeter per test location and the percentage of the European norm.

#	Test locations	Street name	Computed infiltration capacity	Percentage of E-norm
1	Almere 1	Centaurenstraat	27.3	0.28
2	Almere 2	Apollostraat	11.5	0.12
3	Almere 3	Homeruslaan	10.1	0.10
4	Beverwijk 1	Halve Maan (Noorder)	48.2	0.50
5	Beverwijk 2	Halve Maan (Zuider)	36.0	0.37
6	Breda/Effen	Baanakker	45.3	0.47
7	Delft	Drukkerijlaan	40.7	0.42
8	Dussen 1	Groot Zuideveld (1)	81.0	0.83
9	Dussen 2	Groot Zuideveld (2)	90.0	0.93
10	Egmond aan Zee	Julianastraat	25.9	0.27
11	Goirle 1	Sporenring (1)	176.4	1.81
12	Goirle 2	Sporenring (2)	104.4	1.07
13	Rotterdam 1	Hoevestraat	39.6	0.41
14	Rotterdam 2	Harddraverstraat	74.2	0.76
15	Rotterdam 3	Baljuwplein	49.7	0.51
16	Rotterdam 4	Hoekersingel (1)	110.9	1.14
17	Rotterdam 5	Hoekersingel (2)	62.6	0.64
18	Rotterdam 6	Hoekersingel (3)	89.3	0.92
19	Rotterdam 7	Hoekersingel (4)	141.9	1.46
20	Utrecht	Brasemstraat	46.8	0.48
21	Zwolle 1	Pieter Zeemanlaan	226.4	2.33
22	Zwolle 2	Beukenallee	126.0	1.30
23	Zwolle 3	Groeneweg	248.4	2.56
24	Zwolle 4	PC Hoofdstraat	212.4	2.19

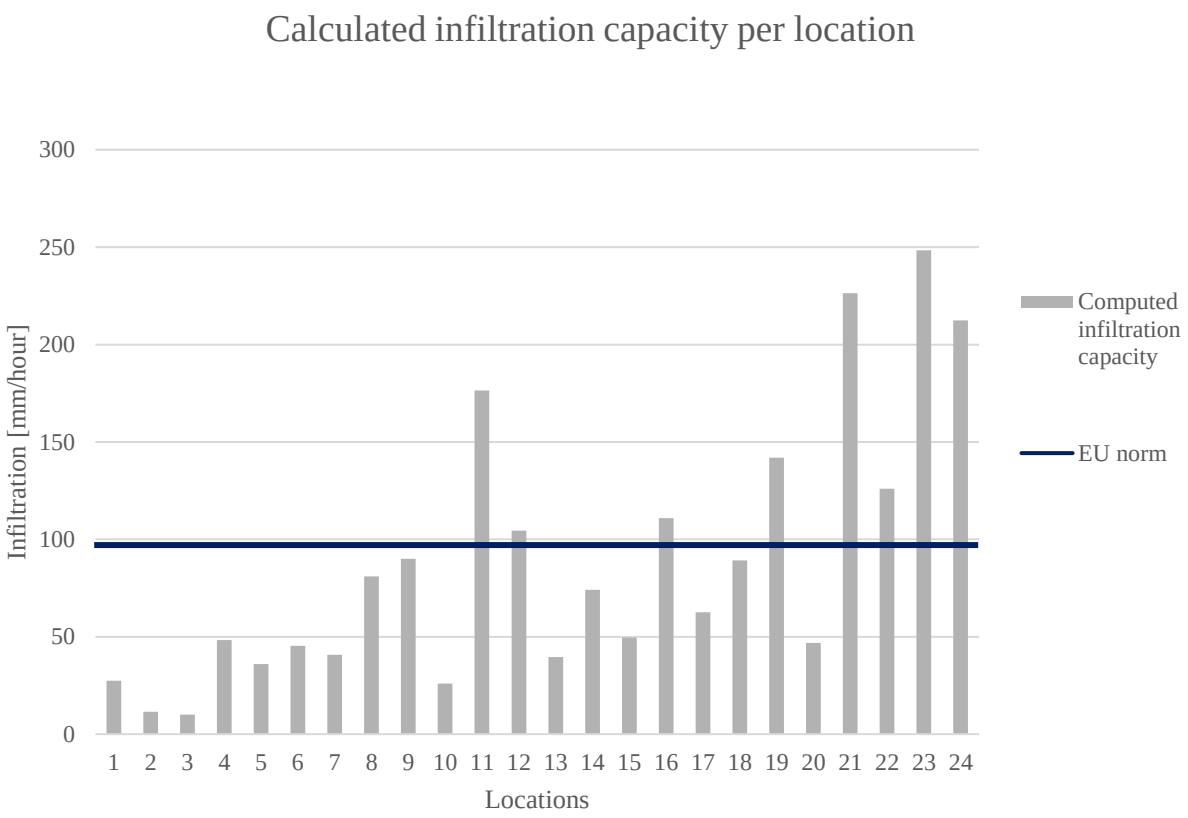

Figure 12: Calculated infiltration capacity per test location and the European norm.

4.3 Analyses

In the previous chapter, the results of the calculations were described. The difference in infiltration capacity of the various permeable pavement surfaces was large. However, it is impossible to make conclusions from the infiltration capacities calculated in previous chapter alone. This chapter describes the analysis that has been performed in order to provide information to undergird the relation between these factors and failure. Underneath, for the total of nine variables, graphs as well as a correlation analysis explain the relation between design and failure of the twenty-four surfaces. If no design information was included, for the three locations in Almere, it was

categorized as ‘Unknown‘. The numbers within each block shows the total count used to compute the average.

Age

Figure 13, show the averaged computed infiltration capacity per age and it shows that the infiltration capacity is highly dependent on the amount of time the structure has been in use. For instance according to the graph), permeable surfaces that were constructed two years before the experiments showed highest infiltration capacities. Those tested after 5 years showed the second lowest value. Permeable pavement surfaces with an age of 1, 4, 5 and 7 show average infiltration capacities under the European norm.

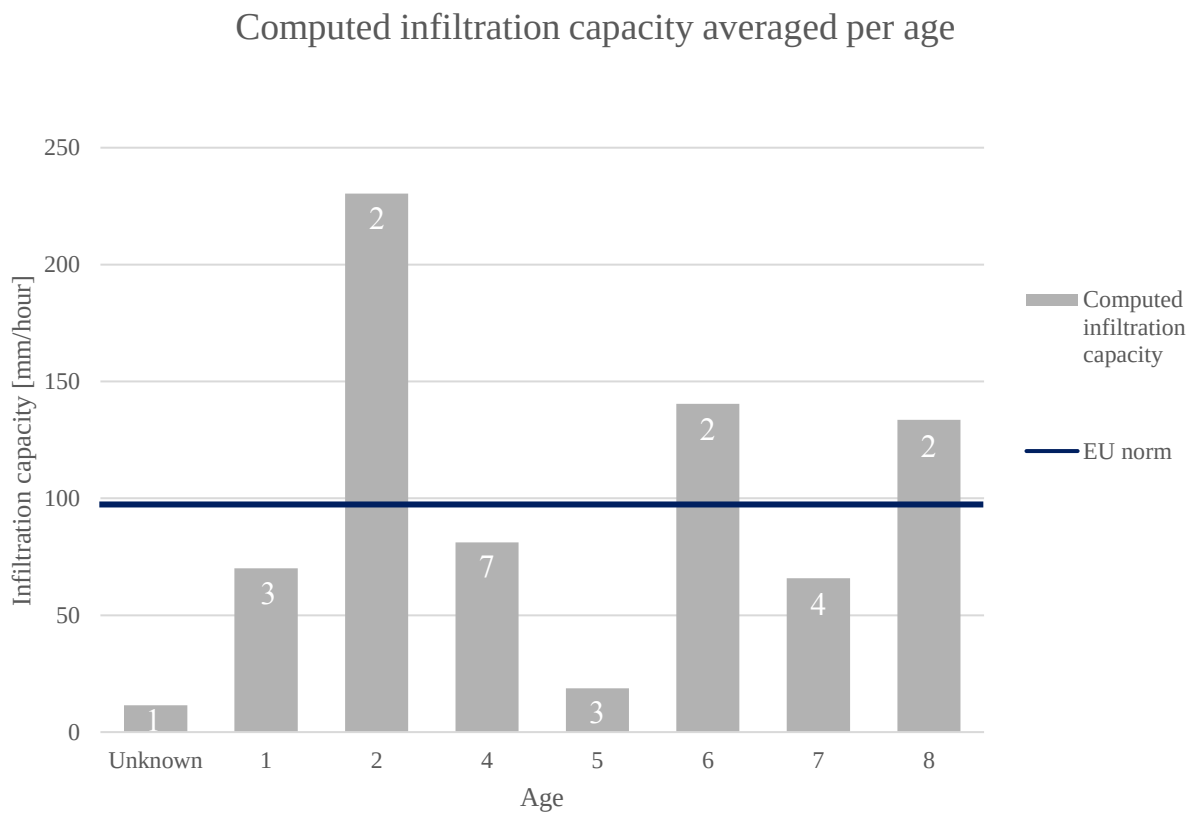

Figure 13: Computed infiltration capacity averaged per age.

Manufacturer

In Figure 14, the average infiltration capacity per manufacturer is shown. From the block chart we can learn that there is a great difference between various manufacturers. Namely, structures constructed by Struyck Verwo and Van den Bosch show relative high infiltration capacities. Structures from Bylandt CRA, Bylandt Drainflow, Holcim Porodur, HUWA, and MIN show infiltration capacities lower than the European norm where MIN and 'Unknown' show the lowest infiltration capacity.

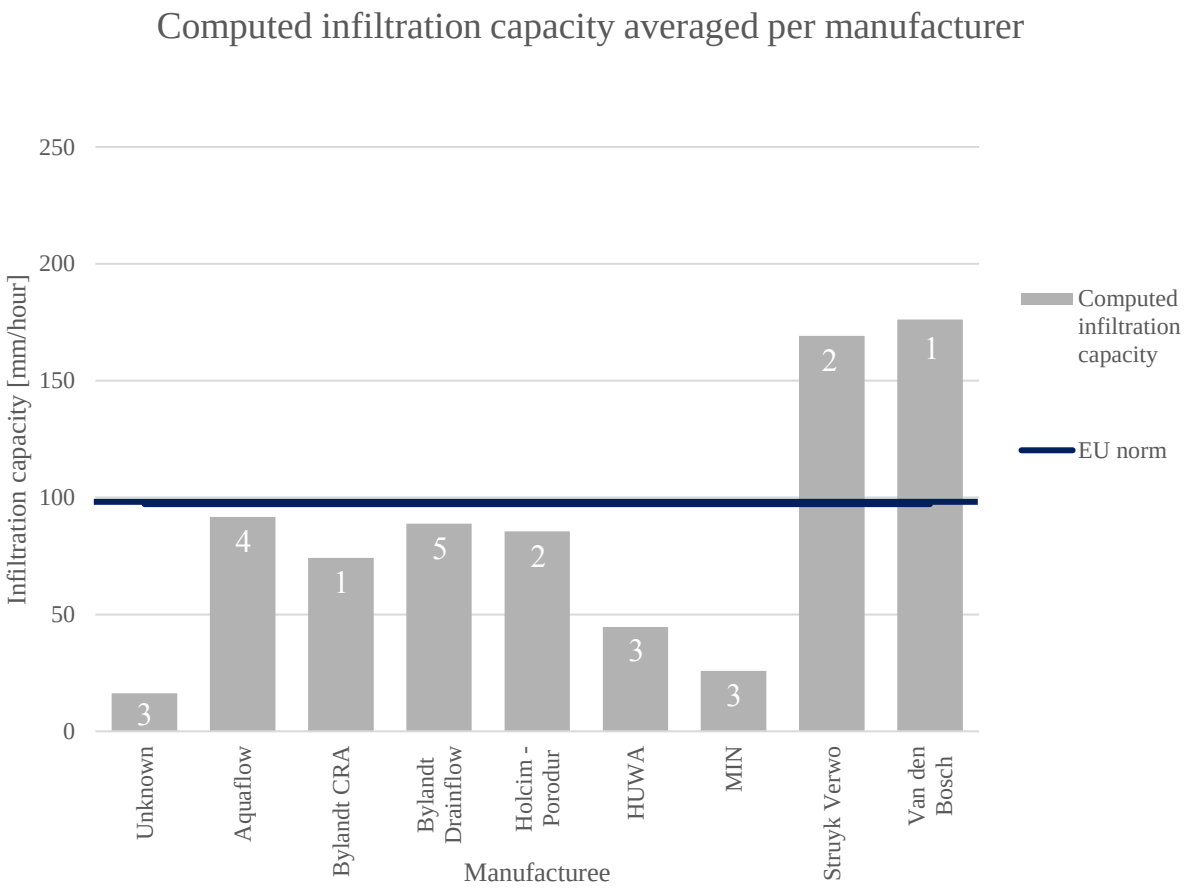

Figure 14: Computed infiltration capacity averaged per manufacture.

Curved surfaces

Whether a curved surface is influencing the extent on which permeable pavement surfaces show reduced infiltration capacities is listed in Figure 15. Based on the information given in the figure, surfaces where no curve is originally constructed show higher infiltration capacities than those that were implemented with a curve. This ratio is roughly between one-third and a-half.

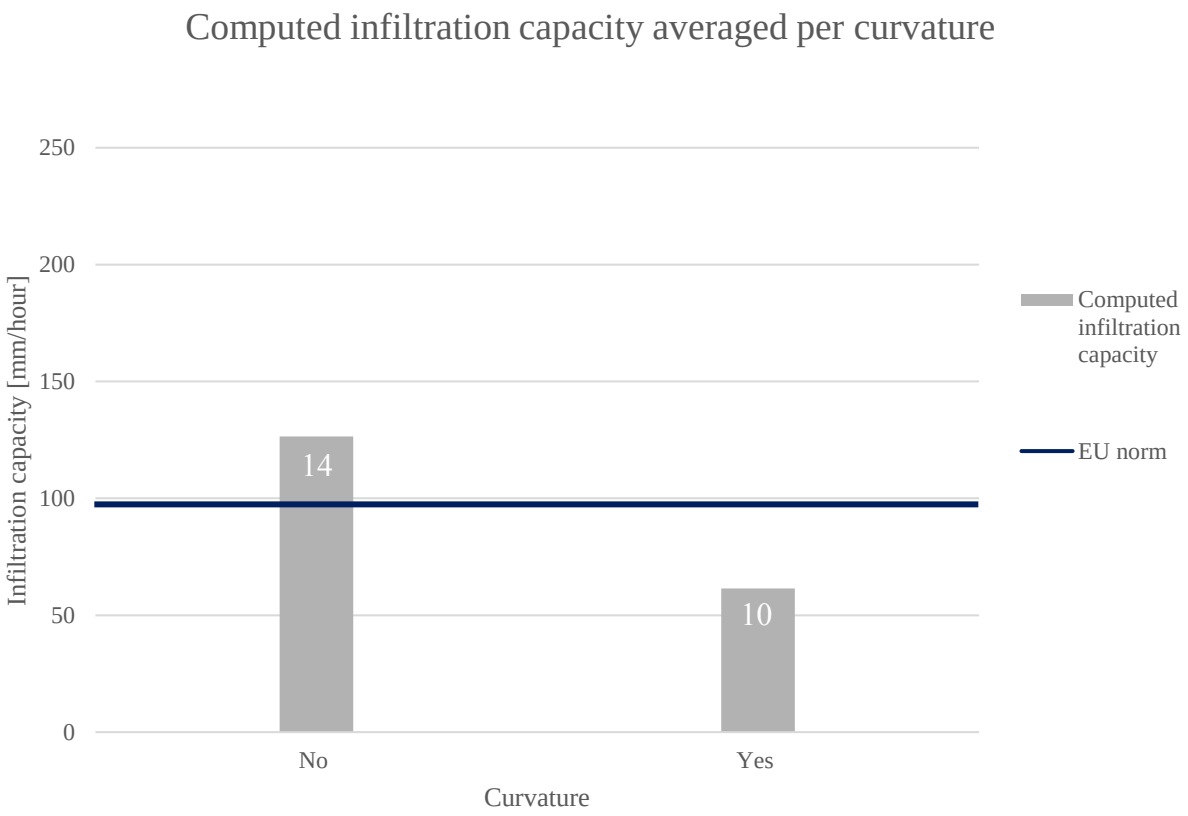

Figure 15: Computed infiltration capacity averaged per curvature.

Filling material

Figure 16 shows the average infiltration capacity per filling material used within the various permeable pavement surfaces. Split 1/3 and 2/6 show relative high averaged infiltration capacities

(around 140 mm/hour) where crushed sand and broken natural stone show the lowest values (around 45 mm/hour). Additionally, single felt shows a value under the European norm.

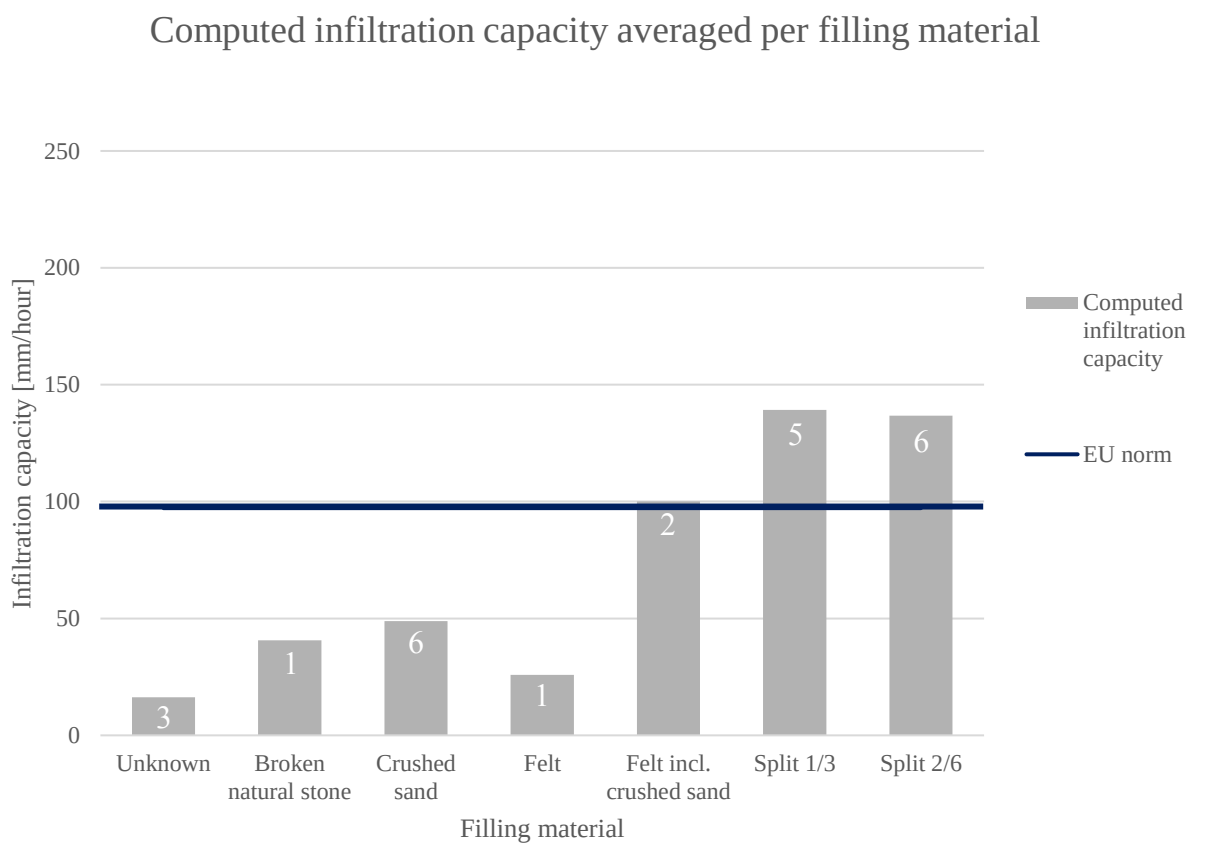

Figure 16: Computed infiltration capacity averaged per filling material.

Joint width size

Figure 17 shows the averaged infiltration capacities for the various joint width size used. A width of 5 millimeter shows the highest averaged infiltration capacity (around 225 mm/hour) where, in addition to the unknown size, 4 millimeter shows the lowest value just under 50 mm/hour.

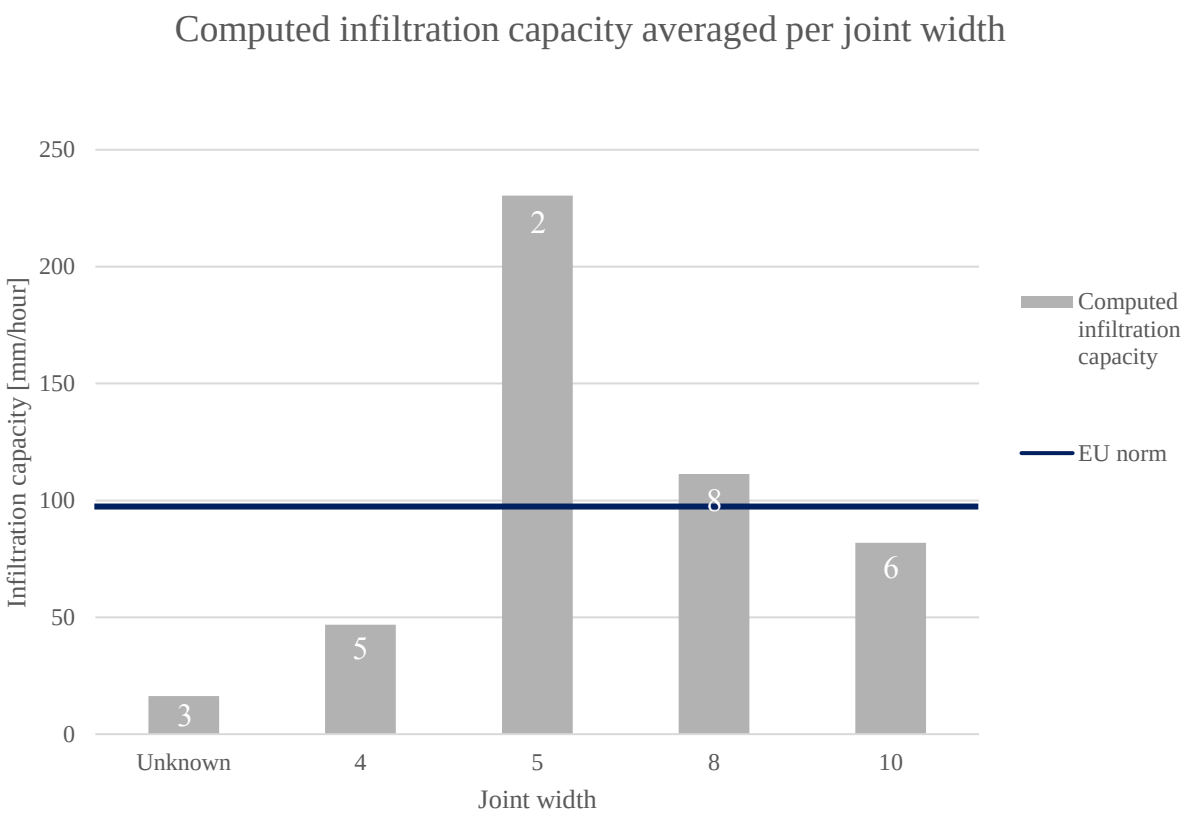

Figure 17: Computed infiltration capacity averaged per joint width size.

Type of lacing

In Figure 18, the average infiltration capacity per lacing material is visualized. The materials ‘broken natural stone’, ‘split 2/6’, and ‘none’ show the highest averaged infiltration capacities. The permeable surface without a specific lacing was construction on top of a sandy soil. This soil type usually has a high permeability. Crushed sand however, shows only around 50 mm/hour on average. Again, ‘Unknown‘ shows the lowest infiltration capacity.

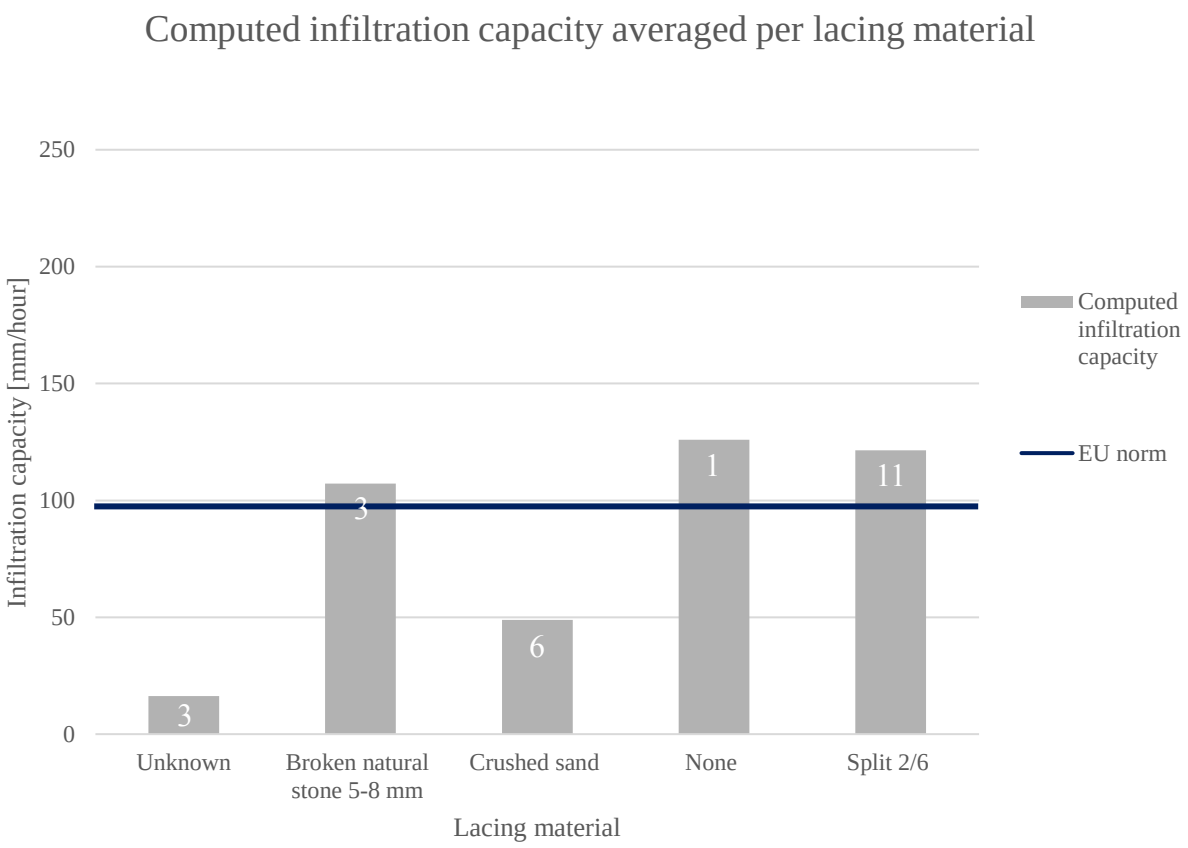

Figure 18: Computed infiltration capacity averaged per lacing material.

Geo-textile

Figure 19 shows that permeable pavement surfaces without any geo-textile included show, on average, higher infiltration values with over 100 mm/hour more than those with a geo-textile. Constructions with geo-textile show less than 80 mm/hour on average.

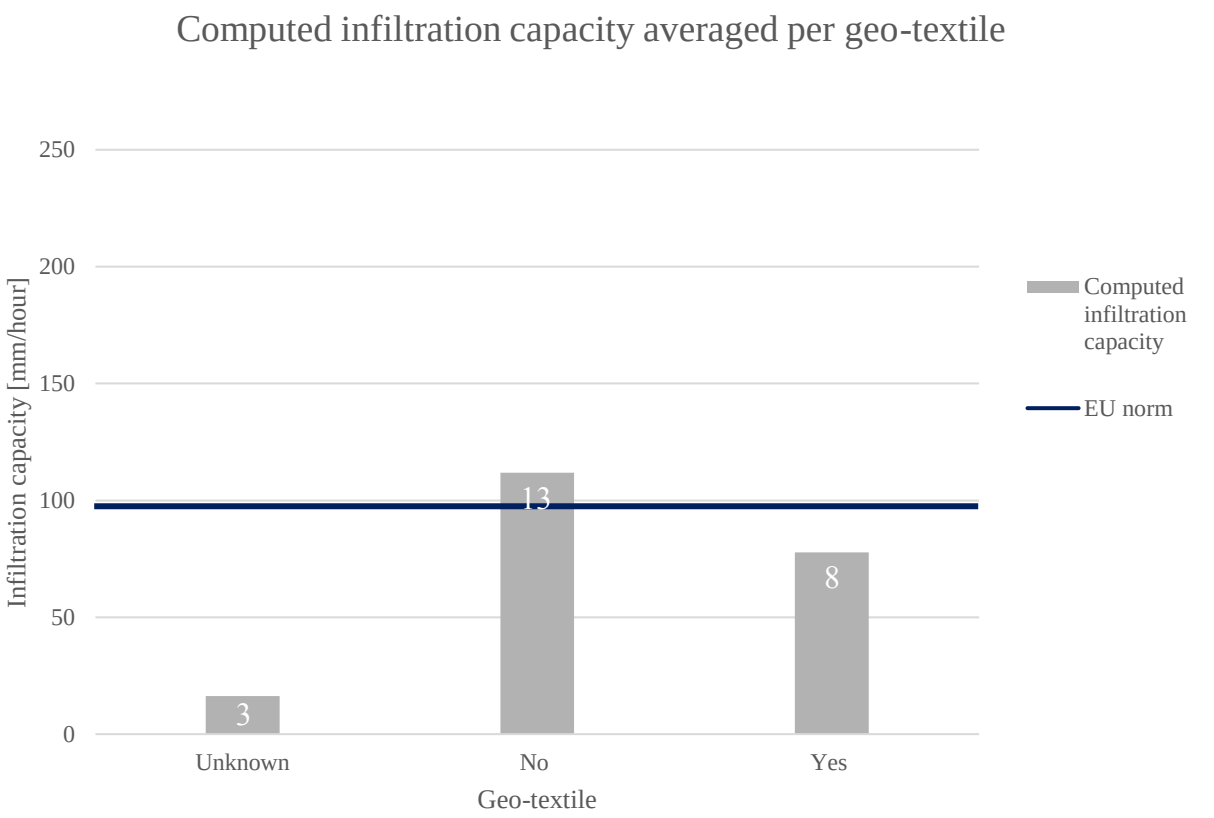

Figure 19: Computed infiltration capacity averaged per implementation of geo-textile.

Buffer layer

In Figure 20, the averaged infiltration capacities per buffer material are visualized. The surfaces where no additional buffer space is created and where the surface is directly implemented on top of the soil underneath shows highest values reaching double the amount required to meet the European norm. Second highest value occurs for surfaces for which additional buffer is created by the deposit of sand. ‘Concrete granulate’, ‘broken natural stone’, and ‘lava’ show values lower than the European norm.

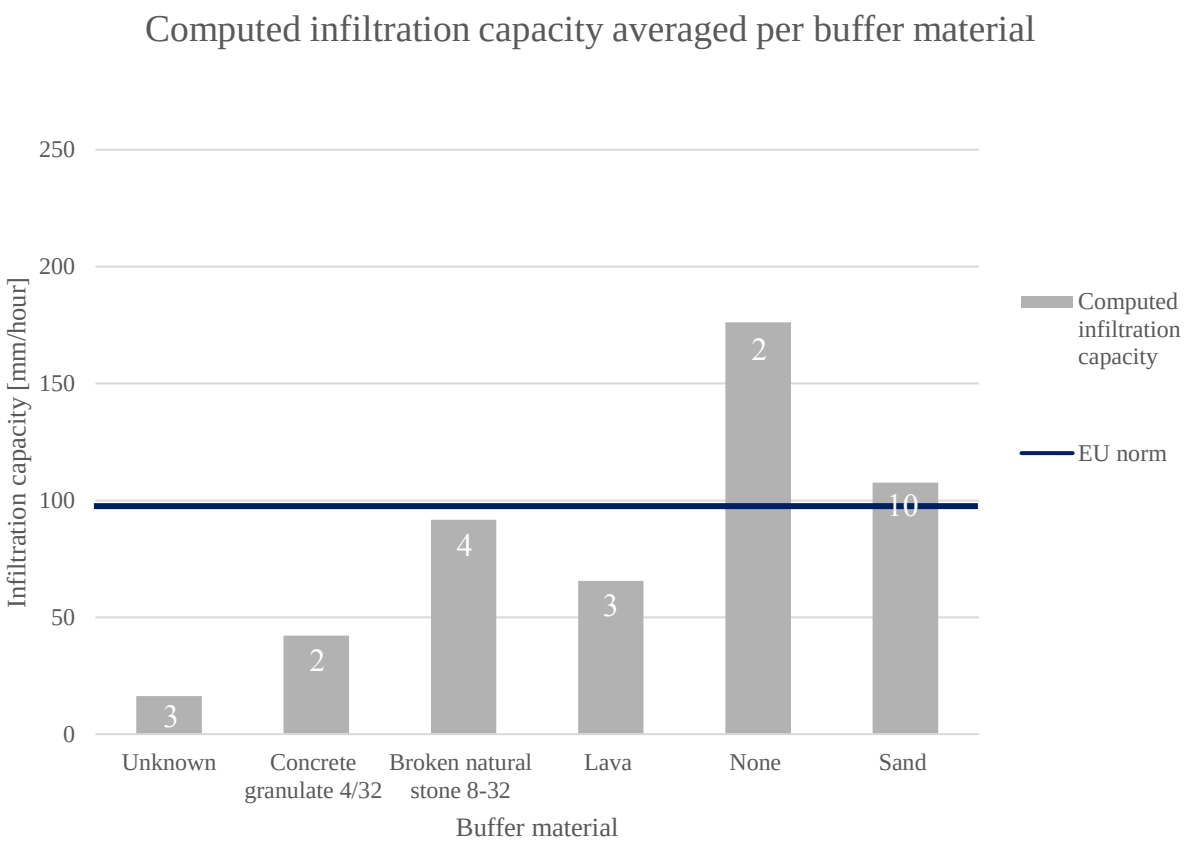

Figure 20: Computed infiltration capacity averaged per buffer material.

Soil type

Figure 21 shows the averaged infiltration capacities per soil type. Constructions implemented on soil consisting of clay show the lowest average infiltration value, just over 20 mm/hour. Other soil types show values fairly similar to each other, around 80 to 100 mm/hour.

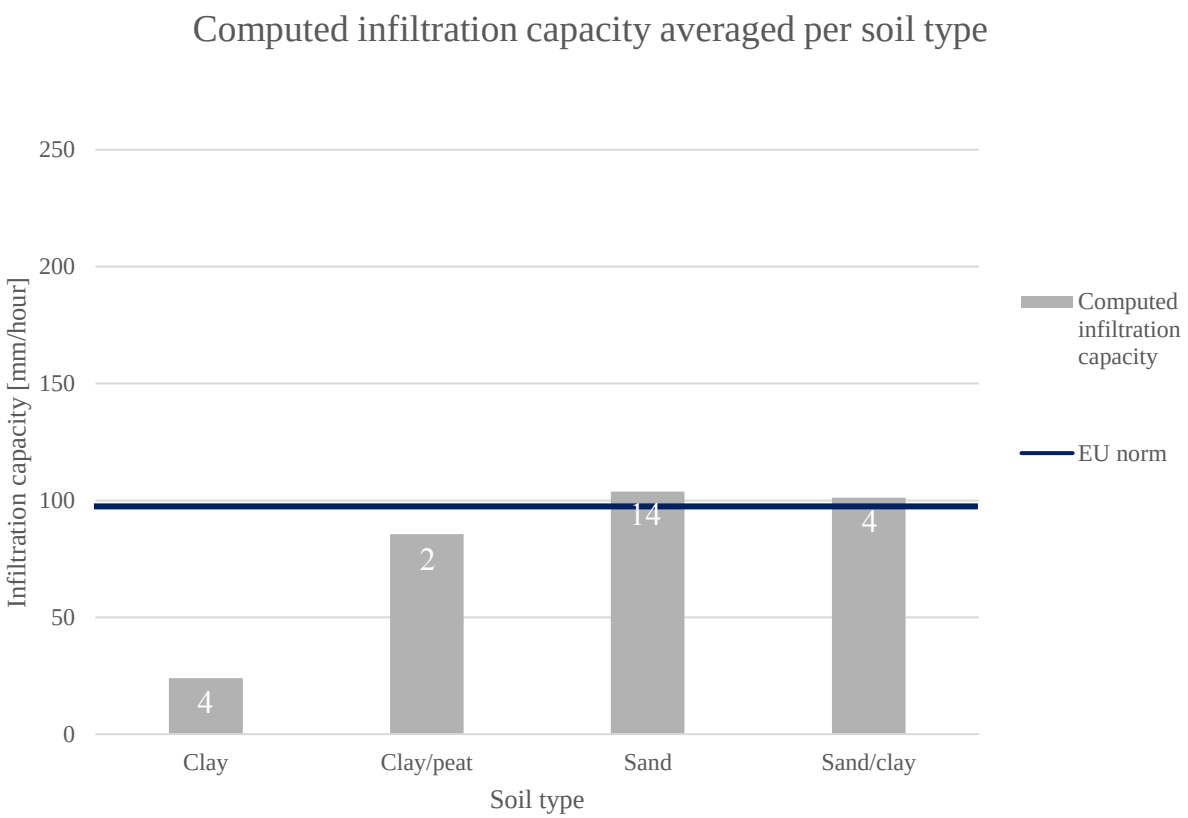

Figure 21: Computed infiltration capacity averaged per soil type.

Environment

Finally, Figure 22 shows the average infiltration capacities per environment type. Permeable pavement surfaces surrounded by medium green environment show infiltration capacities of 80 mm/hour on average. Surfaces within an environment with a high green value show slightly higher average infiltration capacities.

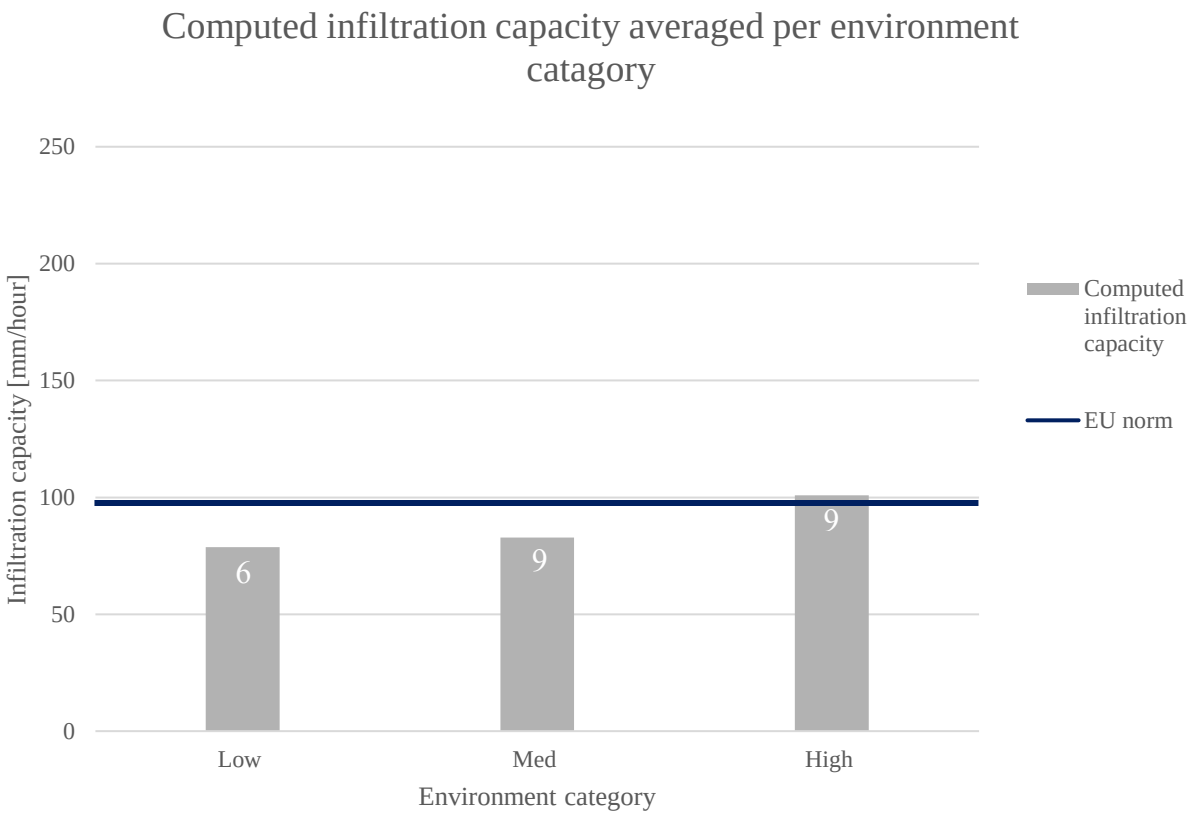

Figure 22: Computed infiltration capacity averaged per environment type.

Correlation

The results of this analysis are given in Table 3. Overall, the results show that the correlation of the individual design and environmental aspects range from -0.11 (lowest amount of correlation) to 0.54 (highest amount of correlation) with an average of 0.34. The manufacture, joint width, and lacing material are showing highest correlation. Age, geo-textile, soil type, and environment show lowest correlation.

Table 3: Computed correlation between design element and infiltration capacity.

Data analyses	**Correlation**
Age	-0.11
Manufacturer	0.51
Curvature	0.48
Filling material	0.39
Joint width	0.54
Lacing material	0.53
Geo-textile	0.25
Buffer material	0.41
Soil type	0.24
Environment	0.14

5. Discussion

5.1 Interpretations of the results

How significant are infiltration capacities after hydrological variables are taken into account?

The methodology of this research shows that when the hydrological variables are included, infiltration capacities calculated show lower results than the method that is currently used. With the new method, for each of the 24 locations the infiltration capacity was calculated within the last centimeter to minimize the influence of the water content of the pores and water pressure. The infiltration capacity calculated with this new method was approximately corresponding with Horton's (1941) equilibrium infiltration rate 'f_c'. Shaffer et al. (2009) stated that clogging is very rarely sufficient to stop water from draining through the surface, faster than it falls onto it. However, the results in Table 2 and Figure 12 show that in many cases the infiltration capacities are in many cases below the European norm of 97.2 millimeter per hour. Therefore, many of the permeable pavement surfaces can be classified as an insufficient solution for storm water management. The significance of the overall infiltration capacities are after hydrological variables are taken into account is therefore low. This is in line with Al-Rubaei et al. (2013), Cipolla et al. (2016), and Kumar et al. (2015) claimed that infiltration capacities significantly dropped after years of implementation. In addition, the results support van Oosterwijk et al. (2015), Wentink (2016), and Stamsnijder (2017) claiming that clogging happens to be a well-known issue making it unclear how long permeable surfaces remain efficient.

Do different types of permeable pavement surfaces show significant reduced infiltration capacities?

From studying the block charts described in the results it can be noticed that variations in elements used in the different types of permeable pavement surfaces show different average infiltration capacities. For instance, when studying Figure 19 showing the averaged infiltration capacities per implementation of geo-textile, infiltration capacities show lower infiltration values when such textile is implemented. This implies that a geo-textile enhances the order in which a permeable pavement surface show results of clogging.

As is described previously in the interpretation of the results, the age of permeable pavement surfaces tends to influence the order in which the constructions show low infiltration capacities (Al-Rubaei et al., 2013; Cipolla et al., 2016; Kumar et al., 2015). However, when studying the averaged infiltration capacities per age in Figure 13, the block chart shows differently characteristics. Namely, there is no linear trend visible indicating the theory that with age, infiltration capacities drop. Moreover, the average infiltration capacity for one-year old structures even belong to the lowest infiltration capacities calculated. The fact that the calculated infiltration capacities show somewhat expected and unexpected results may indicate that some design or environmental aspects are influencing the infiltration capacity more than others, or it may indicate that there is inter-correlation between the various aspects.

Moreover, when studying the averaged infiltration capacities per joint width stated in Figure 17, the results may seem questionable. As the width of the joints increases, the total permeable surface does increase also. A larger permeable surface leads to more water that can infiltrate (Nortier et al., 1996) (although the results in the figure do not correspond with this theory completely). Again, this may indicate that there is inter correlation between the various aspects.

From the figures described in the analysis section it can be considered that various elements show better results than other. The individual correlation of the various design and environmental aspects are explained in Table 3. The results in this table show higher correlation between some aspects than others. The higher correlations might be indicating a higher influence on permeable pavement surfaces, showing reduced infiltration capacities. Based on this information, recommendations can be made in terms of the most promising option for future implementation of permeable pavement surfaces. However, whether a specific construction type or set of elements can be described as most promising is difficult. The reason for this is the low count of variables which the analysis is based on. This is further described under subsequent section 'Limitations'.

5.2 Limitations

In an ideal situation, the direct influence of one aspect on the infiltration capacity is studied in experiments in which all other possible causes of variation are eliminated. The degree of correlation between two variables can be calculated by well-known methods, but when correlation is found it merely gives the resultant of all connecting paths of influence (Wright, 1921). Due to the complexity of permeable pavement surfaces, there are aspects that correlate with each other because they might interact. This is the case with the results of this research. Correlation found during the analysis may show individual relationships between aspects and low infiltration capacities, but the results remain obscure because of the possible multiple interactions between the various elements within one construction. Moreover, the data used in this research was originated and provided by multiple sources. Methods, seasonal variations, and other uncontrollable variables may have had its influence on the outcome of this research increasing the doubt of the result.

In addition, the sample size used during this research is also reason to argue the validity of the results. The infiltration capacity was computed for a total of 24 locations which is a fair amount to study the overall performance of permeable pavement surfaces. However, this amount was relatively low to perform further analysis on the correlation between design or environmental aspects and the infiltration capacities. Among many researchers, using a low sample size is not recommended. Doing so, the finding may show strong correlation even though this is not entirely true. Bujang (2016) proposed a minimum of 29 samples to be used to determine reasonable high correlation of two variables. Since in this research aspects were tested with a sample size lower than 29, the correlations computed have high uncertainties. Since the sample size is low, aspects which normally would show a high correlation if a greater sample size is maintained may now show little correlation or vice versa.

Besides, the results of this thesis show that there is correlation between design and environmental aspects and failure of permeable pavement surfaces showing low infiltration capacities. This only reveals the association between the two variables at the time the experiments were done. It does not provide information about the influences between the independent and dependent variables and thus does not provide knowledge about the functioning in the past nor future. Therefore, since correlation is only the relation between the two variables representing of how closely the two variables co-vary, it cannot be titled as failure mechanism. Namely, a failure mechanism is related to causation (Daley, n.d.). With the use of a causation analysis it is possible to determine the order in which one independent variable is causing the other dependent variable to change. However, in order to do such an analysis different approach is needed. For the research on permeable pavement surfaces, specifically, to conduct a causation analysis it is necessary to monitor the structures for a period of time measuring the infiltration capacity. It then is possible to

see the change of capacity under the case specific conditions and relate the degree of reduction to certain aspects, assuming all other aspects are not interrelated. But since this data is not available currently, such analysis could not be performed. Studying the causation between failure and failure mechanism was therefore not achievable.

5.3 Recommendations

Based on the limitations of this research, the following recommendations are made;

- No further implementations of this type of measure until further knowledge proves the functioning to be sufficient for storm water resilience for a long period.
- For future research it is recommended to study permeable pavement surfaces in controlled environment to test the various aspects separately to exclude uncontrollable influences.
- For future research it is recommended to study permeable pavement surfaces occasionally to get insights on the functioning through time. This improves knowledge on the cause of failure, in combination with previous recommendation.

5.4 Relevance

Before this thesis was initiated, some earlier research on permeable pavement surfaces was already performed. However, unlike these previous studies, this thesis did expand research regarding the full set of permeable pavement surfaces constructed and tested in the Netherlands. In addition, no other type of correlation or causation analysis could be performed on the current set of data. Therefore, the results of this study submits new insights about the current performance of the permeable pavement surfaces in general, recommending more research to be done into the

functioning of such surfaces or alternative measures before further implementation. This thesis shows that the greater amount of permeable pavement surfaces tested aren't functioning conform the European norm, even after a couple of years. This information can be used to substantiate against plans for the implementation of this type of measure. In addition, the results of this thesis provide and substantiate an improved calculation method for storm water resilience which can be used in future research. This method improves the ability to test the permeable pavement surfaces for worst-case scenarios.

6. Conclusions

The main topic of this thesis is the failure of permeable pavement surfaces. During this research, the goal was to analyze possible failure mechanisms behind the failure of such surfaces, in order to achieve understanding about future practices. This thesis shows that the greater amount of permeable pavement surfaces tested aren't functioning conform the European norm. In addition, this thesis provide and substantiate an improved calculation method for storm water resilience which can be used in future research. Namely, this method improves the ability to test the permeable pavement surfaces under certain hydrological conditions, for worst-case scenarios also.

This research included a literature review that was executed leading to the justification of a new calculation method. This review showed that previous results from earlier papers were of insufficient value to be directly used as foundation for the purpose of this thesis. Therefore, in the methodology a new calculation method was designed. The results of this calculation method showed lower infiltration capacities than the method used before. The first hypothesis (H1), whether with realistic hydrological variables during simulations infiltration capacities show reduced values relative to current values, is therefore confirmed.

The results of the new calculations showed that in many cases, the infiltration capacity was insufficient for the permeable pavement surfaces to meet the European norm of 97.2 millimeter per hour. The results of the analyses showed that some individual design and environmental aspects showed correlation between the phenomenon of low infiltration capacities. The second hypothesis of this research stated that the type of permeable pavement surface is determining the order on which the structure shows effects of clogging as reduced infiltration capacities. The results of the correlation analysis explain a slight variation in correlation between the various design and

environmental aspects and the degree of failure of the permeable pavement surfaces. The results therefore confirm the second hypothesis (H2).

However, the results showed only none to moderate correlation and not a single strong correlation between failure and failure mechanism. It can therefore be concluded that certain structural or environmental aspects are correlated with the reduced infiltration capacities, but none can be described as true failure mechanism of failing permeable pavement surfaces. With this information, the main research question of this thesis "*Is there a correlation between the magnitude of failure and failure mechanism of permeable pavements?*" can be answered. Namely, there is no strong correlation between the failure of permeable pavement surfaces and the studied failure mechanism. However, the results show that certain aspects have higher correlation than others which increases the probability to be correlated with the failure of the permeable pavement surfaces. Although, the true cause that negatively affects the infiltration capacities of permeable pavement surfaces should be studied in future research and/or different measures for storm water management should be considered in future urban storm water strategies.

References

Al-Rubaei, A. M., Engström, M., Viklander, M., & Tobias-Blecken, G. (2013). *Long-term hydraulic performance of stormwater.* NOVATECH.

Aquabase. (n.d.). Retrieved from https://www.aquabase.info/kenmerken/ecopass-stenen/

Beeldens, A., & Herrier, G. (2006). *Water Pervious Pavement Blocks: The Beglian Experience.* Brussels: Belgian Road Research Centre.

Boogaard, F., Lucke, T., van de Giesen, N., & van de Ven, F. (2014). *Evaluating the Infiltration Performance of Eight Dutch Permeable Pavements Using a New Full-Scale Infiltration.* Department of Water Management, Tauw bv, NoorderRuimte, Stormwater Research Group, Deltares.

Boogaard, F., Lucke, T., Wentink, R., Dierkes, C., & Akkerman, O. (2015). *International study on the long-term efficiency of stormwater infiltration by permeable pavements.* Hanze University of Applied Sciences, Stormwater Research Group, University of the Sunshine Coast, Tauw bv.

Bujang, M. A., & Baharum, N. (2016). Sample Size Guideline for Correlation Analysis. *World Journal of Social Science Research*, 37-46.

California Department of Transportation. (2014). *Pervious Pavements Design Guidance.* Sacramento: Calidornia Department of Transportation. Division of Design. Office of Storm Water Management.

Castro, D., González-Angullo, N., Rodríguez, J., & Calzada, M. (2007). *The influence of paving-block shape on the infiltration capacity of permeable paving.*

Cipolla, S. S., Maglionico, M., & Stojkov, I. (2016). *Experimental Infiltration Tests on Existing.* Bologna: School of Engineering and Architecture, University of Bologna.

Daley, D. (n.d.). *Failure Modes and Failure Mechanisms.* Continuing Education and Development.

Debye, P. H., Anderson, H. R., & Brumberger, H. (1957). *Scattering by an Inhomogeneous Solid. II. The Correlation Function and Its Application.*

Diver Water Level Data Logger. (2018). Retrieved from https://diver-water-level-logger.com/en/diver-water-level-loggers/

Eijkelkamp. (n.d.). *Product Manual, TD-Diver & Baro-Diver - DI8xx Series.*

Finn, R. (1999). Capillart Surface Interfaces. *Notices AMS*, 770-781.

Fitts, C. R. (2013). *Groundwater Science.* Elsevier.

Google Maps. (2018). Retrieved from Google Maps: https://www.google.com/maps/@52.0324948,5.2219227,8z

Gray, D. M., & Norum, D. I. (1967). *The Effect of Soil Moisture on Infiltration as Related to Runoff and Recharge.* National Research Coucil of Canada.

Horton, R. E. (1941). *An Approach Toward a Physical Interpretation of Infiltration-Capacity.*

Intergovernmental Panel on Climate Change. (2007). *Climate Change 2007: Impacts, Adaptation and Vulnerability.*

Kader, K. H. (2015). *Review on Permeable Pavement Systems.* Bhopal: Department of civil engineering.

Kalmikov, I. V. (2010). *Thermopedia*. Retrieved from Capillary Action: http://www.thermopedia.com/content/31/

Kumar, K., Kozak, J., Hundal, L., Cox, A., Zhang, H., & Granato, T. (2015). *In-situ infiltration performance of different permeable pavements in a employee used parking lot e A four-*

year study. Monitoring and Research Department, Metropolitan Water Reclamation District of Greater Chicago.

Li, H. (2013). Comparative field permeability measurement of permeable pavements using ASTM C1701 and NCAT permeameter methods. *Journal of Environmental Management*, 118C:144-152.

Lucke, T., Beecham, S., Boogaard, F., & Myers, B. (2013). *Are Infiltration Capacities of Clogged Permeable.* NOVATECH.

Lucke, T., Boogaard, F. C., & van der Ven, F. (2014). *Evaluation of a new experimental test procedure to more accurately determine the surface infiltration rate of permeable pavement systems.* Routledge.

Mukaka, M. M. (2012). tatistics Corner: A guide to appropriate use of Correlation coefficient in medical research. *Malawi Medical Journal*, 69-71.

Nortier, I. W., & de Koning, P. (1996). *Toegepaste Vloeistofmechanica.* Stam Techniek.

PDOK. (2018). Retrieved from http://pdokviewer.pdok.nl/

Qianqian, Z. (2014). *A Review of Sustainable Urban Drainage Systems Considering the Climate Change and Urbanization Impacts.* School of Civil and Transportation Engineering.

Shaffer, P., Wilson, S., Brindle, F., Baffoe-Bonnie, B., Prescott, C., & Tarbet, N. (2009). *Understanding permeable and impermeable surfaces, Technical report on surfacing options and cost benefit analysis.* Department for Communities and Local Government.

SPSS Handboek. (sd). Opgehaald van https://spsshandboek.nl/manova/

Stamsnijder, E. (2017). *Full scale proef waterpasserende verharding Bijland 5 Tolkamer.* Tauw bv.

Szymkiewics, A. (2013). Chapter 2, Mathematical Models of Flow in Porous Media. In *Modelling Water Flow in Unsaturated Porous Media* (pp. 9-47).

Trenberth, K., Dai, A., Rasmussen, R., & Parsons, D. (2003). *The Changing Character of Precipitation.*

van Oosterwijk, J. M., & Harten, F. J. (2015). *Monitoring waterpasserende verharding Sporenring Goirle. Bepaling infiltratiecapaciteit waterpasserende verharding Sporenring te Goirle.* Tauw bv.

Verwo, S. (n.d.). *Easy Flow, Waterregulerede Bestrating.*

Wang, Q., Shen, Y., & Zhang, J. Q. (2005). *A nonlinear correlation measure for multivariable data set.*

Wegenbouw, O. v. (2008). *Waterdoorlatende verhardingen met betonstraatstenen. Report on pervious pavements.* Brussel.

Wentink, R. (2016). *Onderzoek Aquabase Potgieterstraat te Nijverdal.* Tauw bv.

Wright, S. (1921). *Correlation and Causation.* Senior Animal Husandman in Animal Genetics. Bureau of Animal Insustry.

Zhan, T. L. (2004). *Analytical Analysis of Rainfall Infiltration Mechanism in Unsaturated Soils.* INTERNATIONAL JOURNAL OF GEOMECHANICS.

Appendixes

1. Brief explanation of the double ring infiltrometer test and the full-scale test

During the double ring infiltrometer test, setup illustrated in Figure 23 is used. Two rings are installed on the permeable surface. A substance is added to the bottom of the outer ring to prevent water to spill during experiments. Water is then added to both rings which will infiltrate into the porous media. The reason two rings are used is because water normally not only infiltrates vertically, but also horizontally. In the figure it is illustrated that the water infiltrates from the outer ring not only vertical, but also flows horizontally. Water in the ring in the center of the setup infiltrates mainly in vertical direction as the water from the outer ring prevents horizontal filtration. The data measured in the center ring is therefore gives a fairly reliable indication of the vertical infiltration rate of the porous media.

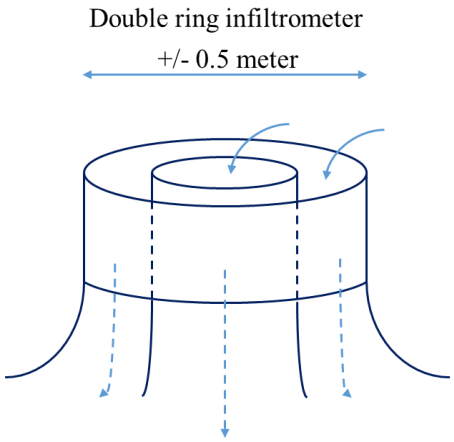

Figure 23: Illustration of double ring infiltrometer test setup.

During the full-scale setup, a larger area is intentionally flooded than the double ring infiltrometer. Usually a street is inundated over the total width over several meters in length, see Figure 24. During these experiments, the curbs of the street acts as wall. For the open ends of the street, temporal dams are constructed to prevent water to flow elsewhere, if no other blockage such as a speed bumps are present.

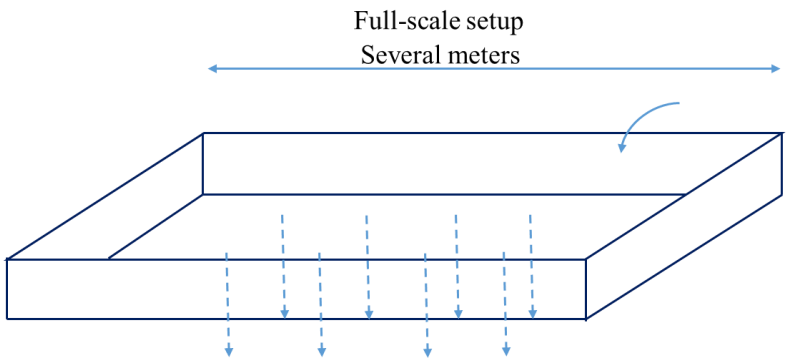

Figure 24: Illustration of full-scale test setup.

During both experiments, infiltration rates are measured in two ways. One is the falling head test, the other the constant head test. During the falling head test, water in added to the setup until a certain water level is reached. Then, the water source is disabled which will result in the water level to drop until the pavement surface is 'dry'. During the experiment, the water level is measured with so called Divers. The Diver, see Figure 25, is placed on the pavement surface and measures the pressure as a result of water height during the experiment. The change of water pressure per period of time can be used to calculate the infiltration rate.

Figure 25: Photo of diver measuring equipment (Diver Water Level Data Logger, 2018).

During the constant head test, water is added to the setup until a certain level is reached. Then, this water level is kept the same for a certain period by tweaking the discharge of the water

source. The discharge needed to keep the water level steady is then noted. This discharge together with the total area of the setup can then be used to compute the infiltration rate.

2. Data collection. Table with information about the permeable pavement surfaces.

#	Test locations	Street name	Age	Manufacturer
1	Almere 1	Centaurenstraat	5	-
2	Almere 2	Apollostraat	-	-
3	Almere 3	Homeruslaan	5	-
4	Beverwijk 1	Halve Maan (Noorder)	1	HUWA
5	Beverwijk 2	Halve Maan (Zuider)	1	HUWA
6	Breda/Effen	Baanakker	7	Aquaflow
7	Delft	Drukkerijlaan	8	Aquaflow
8	Dussen 1	Groot Zuideveld	7	Holcim - Porodur
9	Dussen 2	Groot Zuideveld	7	Holcim - Porodur
10	Egmond aan Zee	Julianastraat	5	MIN
11	Goirle1	Sporenring	6	Aquaflow
12	Goirle2	Sporenring	6	Aquaflow
13	Rotterdam 1	Hoevestraat	4	Bylandt Drainflow
14	Rotterdam 2	Harddraverstraat	4	Bylandt CRA
15	Rotterdam 3	Baljuwplein	4	HUWA
16	Rotterdam 4	Hoekersingel (1)	4	Bylandt Drainflow
17	Rotterdam 5	Hoekersingel (2)	4	Bylandt Drainflow
18	Rotterdam 6	Hoekersingel (3)	4	Bylandt Drainflow
19	Rotterdam 7	Hoekersingel (4)	4	Bylandt Drainflow
20	Utrecht 2	Brasemstraat	7	Struyk Verwo
21	Zwolle 1	Pieterzeemanlaan	8	Van den Bosch
22	Zwolle 2	Beukenallee	1	Van den Bosch
23	Zwolle 3	Groeneweg	2	Struyk Verwo
24	Zwolle 4	PC Hoofdstraat	2	Struyk Verwo

#	Test locations	Street name	Curved surfaces (yes/no)	Filling material
1	Almere 1	Centaurenstraat	Yes	-
2	Almere 2	Apollostraat	Yes	-
3	Almere 3	Homeruslaan	Yes	-
4	Beverwijk 1	Halve Maan (Noorder)	No	Crushed sand
5	Beverwijk 2	Halve Maan (Zuider)	No	Crushed sand
6	Breda/Effen	Baanakker	No	Crushed sand
7	Delft	Drukkerijlaan	No	Broken natural stone
8	Dussen 1	Groot Zuideveld	Yes	Split 2/6
9	Dussen 2	Groot Zuideveld	Yes	Split 2/6
10	Egmond aan Zee	Julianastraat	Yes	Felt
11	Goirle1	Sporenring	No	Split 1/3
12	Goirle2	Sporenring	No	Split 1/3
13	Rotterdam 1	Hoevestraat	Yes	Crushed sand
14	Rotterdam 2	Harddraverstraat	Yes	Crushed sand
15	Rotterdam 3	Baljuwplein	Yes	Crushed sand
16	Rotterdam 4	Hoekersingel (1)	Yes	Felt incl. crushed sand
17	Rotterdam 5	Hoekersingel (2)	Yes	Split 1/3
18	Rotterdam 6	Hoekersingel (3)	Yes	Felt incl. crushed sand
19	Rotterdam 7	Hoekersingel (4)	Yes	Split 2/6
20	Utrecht 2	Brasemstraat	Yes	Split 2/6
21	Zwolle 1	Pieterzeemanlaan	No	Split 1/3
22	Zwolle 2	Beukenallee	No	Split 1/3
23	Zwolle 3	Groeneweg	No	Split 2/6
24	Zwolle 4	PC Hoofdstraat	No	Split 2/6

#	Test locations	Street name	Size of joints single [mm]	Type of lacing
1	Almere 1	Centaurenstraat	-	-
2	Almere 2	Apollostraat	-	-
3	Almere 3	Homeruslaan	-	-
4	Beverwijk 1	Halve Maan (Noorder)	4.00	Crushed sand
5	Beverwijk 2	Halve Maan (Zuider)	4.00	Crushed sand
6	Breda/Effen	Baanakker	8.00	Crushed sand
7	Delft	Drukkerijlaan	8.00	Broken natural stone 5-8 mm
8	Dussen 1	Groot Zuideveld	8.00	Split 2/6
9	Dussen 2	Groot Zuideveld	8.00	Split 2/6
10	Egmond aan Zee	Julianastraat	4.00	Split 2/6
11	Goirle1	Sporenring	8.00	Broken natural stone 5-8 mm
12	Goirle2	Sporenring	8.00	Broken natural stone 5-8 mm
13	Rotterdam 1	Hoevestraat	10.00	Crushed sand
14	Rotterdam 2	Harddraverstraat	4.00	Crushed sand
15	Rotterdam 3	Baljuwplein	4.00	Crushed sand
16	Rotterdam 4	Hoekersingel (1)	10.00	Split 2/6
17	Rotterdam 5	Hoekersingel (2)	10.00	Split 2/6
18	Rotterdam 6	Hoekersingel (3)	10.00	Split 2/6
19	Rotterdam 7	Hoekersingel (4)	10.00	Split 2/6
20	Utrecht 2	Brasemstraat	10.00	Split 2/6
21	Zwolle 1	Pieterzeemanlaan	8.00	Split 2/6
22	Zwolle 2	Beukenallee	8.00	None
23	Zwolle 3	Groeneweg	5.00	Split 2/6
24	Zwolle 4	PC Hoofdstraat	5.00	Split 2/6

#	Test locations	Street name	Geo-textile (yes/no)	Buffer layer
1	Almere 1	Centaurenstraat	-	-
2	Almere 2	Apollostraat	-	-
3	Almere 3	Homeruslaan	-	-
4	Beverwijk 1	Halve Maan (Noorder)	Yes	Concrete granulate 4/32
5	Beverwijk 2	Halve Maan (Zuider)	Yes	Concrete granulate 4/32
6	Breda/Effen	Baanakker	Yes	Broken natural stone 8-32
7	Delft	Drukkerijlaan	Yes	Broken natural stone 8-32
8	Dussen 1	Groot Zuideveld	Yes	Lava
9	Dussen 2	Groot Zuideveld	Yes	Lava
10	Egmond aan Zee	Julianastraat	No	Lava
11	Goirle1	Sporenring	Yes	Broken natural stone 8-32
12	Goirle2	Sporenring	Yes	Broken natural stone 8-32
13	Rotterdam 1	Hoevestraat	No	Sand
14	Rotterdam 2	Harddraverstraat	No	Sand
15	Rotterdam 3	Baljuwplein	No	Sand
16	Rotterdam 4	Hoekersingel (1)	No	Sand
17	Rotterdam 5	Hoekersingel (2)	No	Sand
18	Rotterdam 6	Hoekersingel (3)	No	Sand
19	Rotterdam 7	Hoekersingel (4)	No	Sand
20	Utrecht 2	Brasemstraat	No	Sand
21	Zwolle 1	Pieterzeemanlaan	No	None
22	Zwolle 2	Beukenallee	No	None
23	Zwolle 3	Groeneweg	No	Sand
24	Zwolle 4	PC Hoofdstraat	No	Sand

#	Test locations	Street name	Soil type	Environment
1	Almere 1	Centaurenstraat	Clay	Med
2	Almere 2	Apollostraat	Clay	Med
3	Almere 3	Homeruslaan	Clay	Med
4	Beverwijk 1	Halve Maan (Noorder)	Sand	Low
5	Beverwijk 2	Halve Maan (Zuider)	Sand	Low
6	Breda/Effen	Baanakker	Sand	Med
7	Delft	Drukkerijlaan	Sand	Med
8	Dussen 1	Groot Zuideveld	Clay/peat	Med
9	Dussen 2	Groot Zuideveld	Clay/peat	Med
10	Egmond aan Zee	Julianastraat	Sand	Low
11	Goirle1	Sporenring	Sand	High
12	Goirle2	Sporenring	Sand	High
13	Rotterdam 1	Hoevestraat	Sand	Low
14	Rotterdam 2	Harddraverstraat	Sand	Low
15	Rotterdam 3	Baljuwplein	Sand	High
16	Rotterdam 4	Hoekersingel (1)	Sand/clay	High
17	Rotterdam 5	Hoekersingel (2)	Sand/clay	High
18	Rotterdam 6	Hoekersingel (3)	Sand/clay	High
19	Rotterdam 7	Hoekersingel (4)	Sand/clay	High
20	Utrecht 2	Brasemstraat	Clay	High
21	Zwolle 1	Pieterzeemanlaan	Sand	Med
22	Zwolle 2	Beukenallee	Sand	High
23	Zwolle 3	Groeneweg	Sand	Low
24	Zwolle 4	PC Hoofdstraat	Sand	Med